CHAPTER III

RESULT

Preparation of Various Dispersions

Eighty preparations of HCTZ dispersion and treated HCTZ consisting of pure HCTZ, four treated HCTZ, eighteen physical mixtures, eighteen kneading mixtures, nine solvent mixtures, twelve solvent deposition mixtures, and eighteen ball milling mixtures were investigated.

Most HCTZ dispersions with CT, CS, CSU, LMCS, PVP and PEG were relatively easy to be prepared. Slight difficulty did occur. The solvent method with carrier CT could not use common solvents for preparation. In addition, CS and CSU should be dissolved in acid solution which could not be completely evaporated. Hence the solvent deposition method were additionally investigated. All dispersions obtained were free-flowing powder.

The dispersions of kneading method with LMCS or PVP were brittle and easily pulverized. The PVP KMs obtained were opaque white, while LMCS KMs were yellowish. The PEG KMs were not as brittle. The final product of either CT, CS, or CSU was characteristically the same as before the preparation in grayish to white color.

The dispersions of solvent method with PVP were glassy, transparent, brittle, and easily pulverized. In contrast, the PEG SMs were opaque white waxlike, and slightly difficult to pulverize. The yellowish LMCS SMs were characteristically the same as PVP SMs. Solvent depositions of either CT, CS, or CSU were similar to those before preparation.

The dispersions of ball milling method produced much finer mixtures compared with those before the preparation.

The Calibration Curve

Typical calibration curve for HCTZ data at 272 nm as determined using linear regression is shown in Appendix I (Table 8 and Figure 59). The correlation coefficient for fitting a straight line was significant.

Dissolution Studies of HCTZ Powders

The dissolution profiles of HCTZ from its dispersions and treated HCTZ by different methods of physical, kneading, solvent, and ball milling were given in Figure 10-29 and experimental data are given in Appendix II. The average value of each data was obtained from three determinations at a given sampling time.

All dissolution data and profiles were demonstrated in three categories: firstly, showing the power of increasing carrier ratio (Fig. 11-19); Secondly, comparison of four methods (Fig. 20-25); Finally, comparing the ability of each carrier (Fig. 26-29).

HCTZ

The comparison of dissolution profiles of HCTZ and treated HCTZ; HCTZ, HCTZ PM, HCTZ KM, HCTZ SM and HCTZ BM as illustrated in Figure 10 revealed that HCTZ PM and HCTZ KM exhibited the same pattern and was very slightly different from its pure drug. For HCTZ BM, the percentage of drug dissolved was more during the first 10 minutes and then slightly less than that of HCTZ. Moreover, HCTZ SM exhibited the slowest dissolution profile at each time interval, compared with other dispersion. The resultants from treated HCTZ revealed that no marked increment of HCTZ dissolved except the early stage of HCTZ BM.

Ratio Comparison

Three ratios of 1:1, 1:2, 1:3 drug : carrier were studied in order to compare the results and obtain the suitable ratio. The outcome of each method (PM, KM, SM, BM) showed similar pattern of dissolution profile that increasing in weight fraction of carrier resulted in a corresponding increase in percentage of drug dissolved.

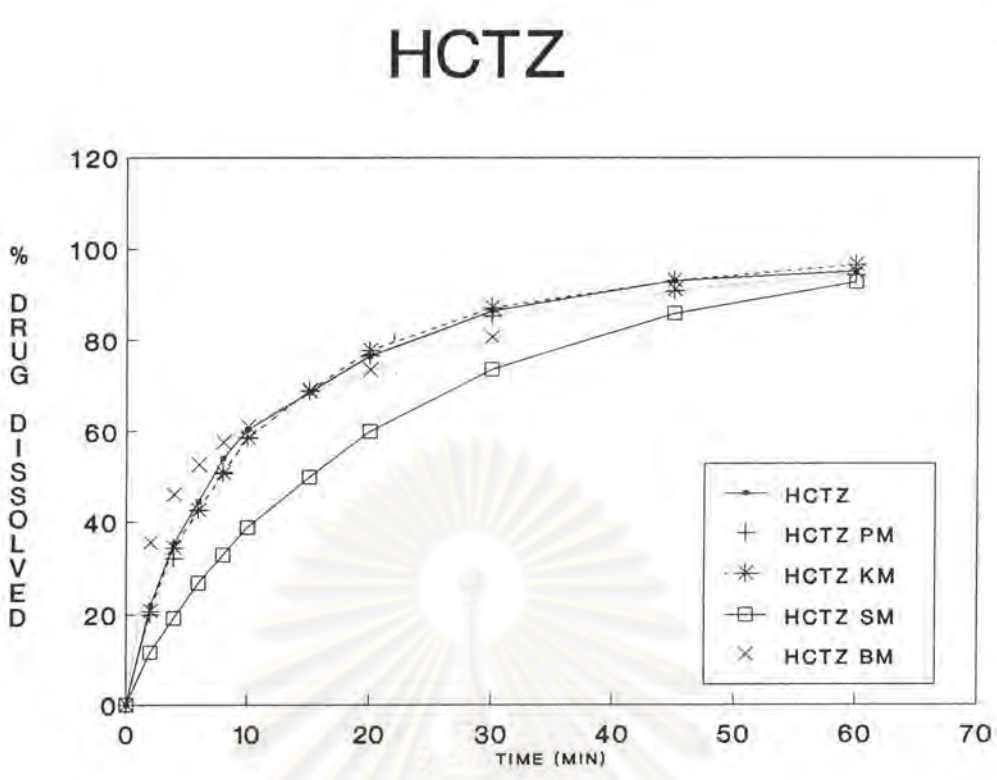

Figure 10 The dissolution profiles of HCTZ from untreated and treated HCTZ powders

In the case of physical method, Figure 11-12, the released profiles of physical mixture of each carrier, CT, CS, CSU and PEG was some what similar to higher carrier ratio which exhibited higher percentage of drug dissolved. Also mixtures of LMCS and PVP except 1:3 ratio was slightly less than those of 1:2 ratio when compared with HCTZ PM or HCTZ, most mixtures exhibited slightly greater dissolution except 1:1 CSU PM and all ratios of PVP PM.

The profiles of kneading method in Figure 13-14 showed that some kneading mixtures exhibited the same dissolution as physical mixture. As for CSU KM and PEG KM the higher the ratio, the higher of HCTZ dissolved. Most kneading mixture showed, in early stage, no difference among three studied ratio. CT KM and PVP KM also exhibited no difference in their dissolution curves between ratio 1:1 and 1:2. Moreover dissolution profile of LMCS KM at every ratio was found to be equal. Difference was noticed in CS KM with the ratio of 1:1 being slightly equal to 1:3 ratio. All kneading mixtures displayed remarkably higher percentage of drug dissolved than HCTZ or HCTZ KM especially with the carriers LMCS and KM.

Systems of solvent method in Figure 15-17 were separated into two groups, by SMD and SM. In SMD, systems of CT, CS, CSU and LMCS differed in dissolution profile. Either CS or CSU showed slightly higher dissolution when increased the amount of carrier. However 1:1 LMCS SMD exhibited higher dissolution than the ratios of 1:2 or 1:3. Also in CT SMD, the percentage of drug dissolution was relatively increased with higher carrier ratio during the first 10 minutes, then the ratios of 1:1and 1:2 showed slightly higher dissolution than the ratio of 1:3. In SM method, LMCS SM exhibited slightly different profile among the three ratios, the ratio of 1:2 exhibited higher dissolution in an early stage then eventually was equal to the ratio of 1:3. For PVP SM and PEG SM, it was obviously shown that the more fraction of carrier the more increase in percent drug dissolved. Most mixtures of both methods (SM, SMD) displayed higher dissolution profile than HCTZ or HCTZ SM, remarkably in LMCS SM. However some ratios of LMCS SMD were apparently not different from untreated HCTZ.

The dissolution profiles of HCTZ from ball milling dispersions in Figure 18-19 showed that most mixtures exhibited slight change in dissolution when the amount of carrier was increased. CT BM, CS BM and PVP BM showed similar dissolution profile that the higher of carrier ratio the higher dissolution profile. LMCS BM of both SW and VB methods exhibited the same dissolution except that 1:1 LMCS BM produced little higher dissolution than other ratios. In contrast, CSU BM showed significant difference from other mixtures. 1:2 CSU BM showed highest dissolution followed by 1:3 and 1:1 ratio. Most mixtures showed markedly increased in drug dissolved

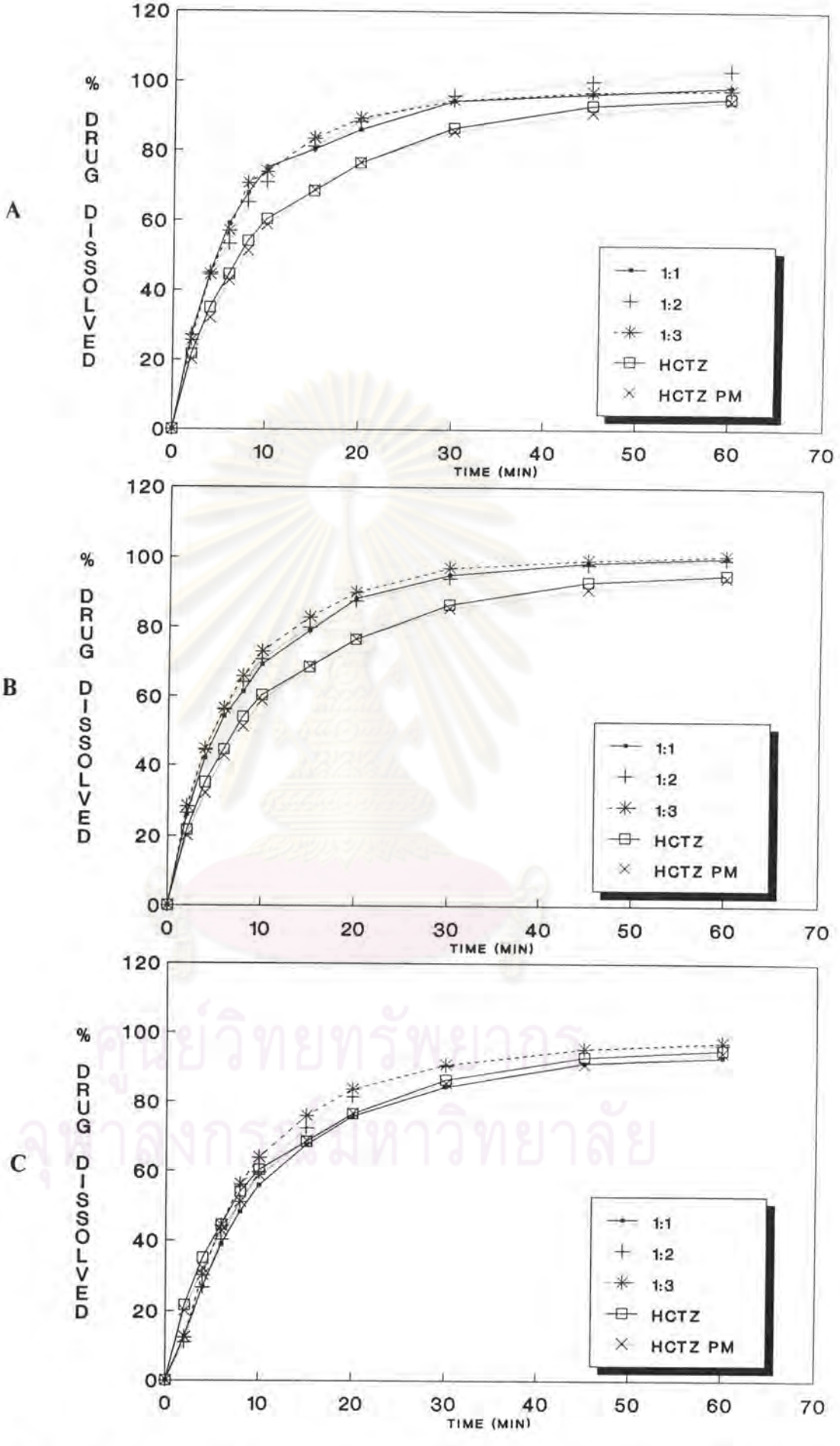

Figure 11 The dissolution profiles of HCTZ physical mixture showing of three ratios (key: A-CTPM , B-CSPM , C-CSU PM)

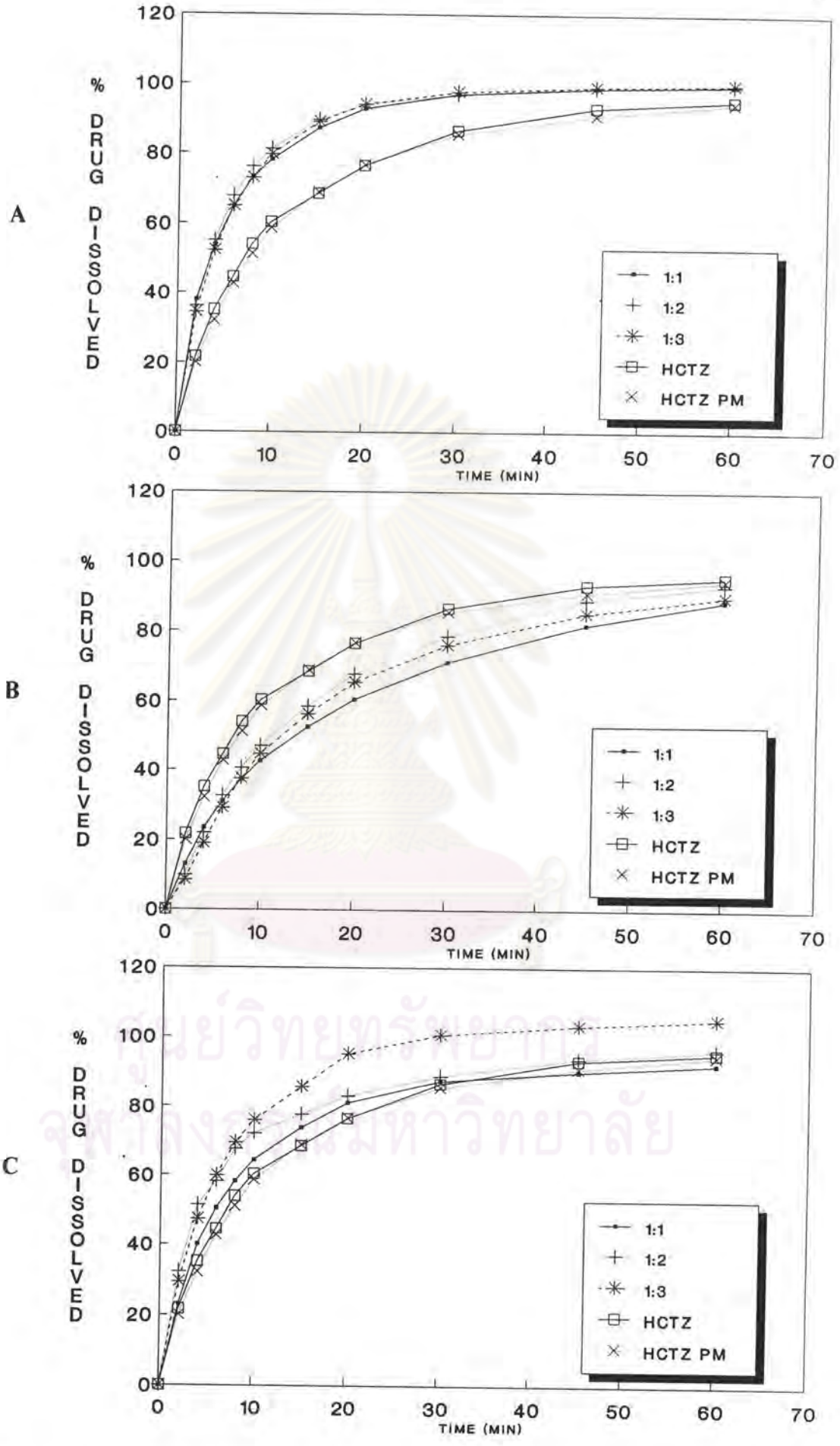

Figure 12 The dissolution profiles of HCTZ physical mixture showing of three ratios (key: A-LMCS PM, B-PVP PM, C-PEG PM)

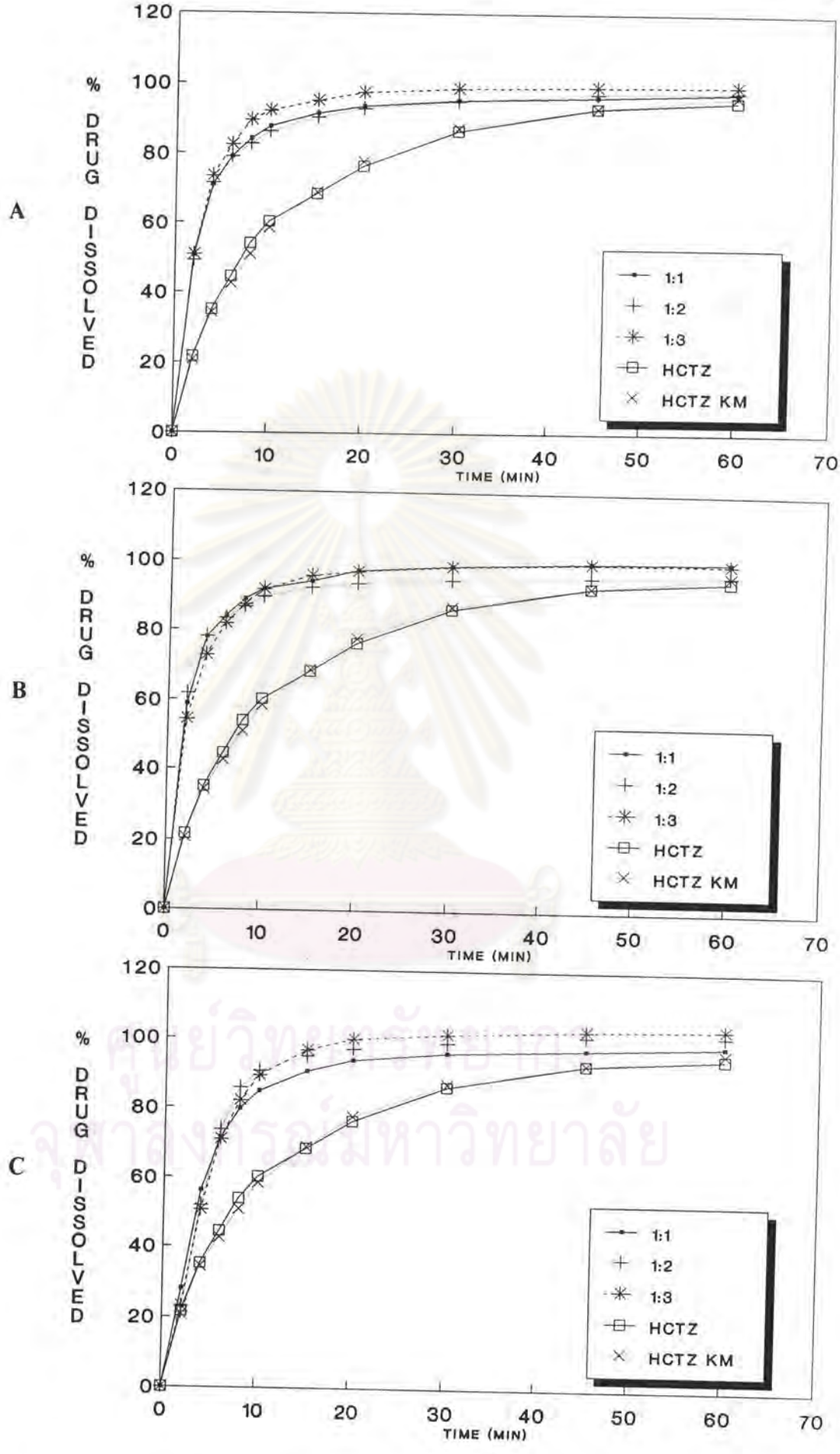

Figure 13 The dissolution profiles of HCTZ kneading mixture showing of three ratios (key : A-CT KM, B-CS KM, C-CSU KM)

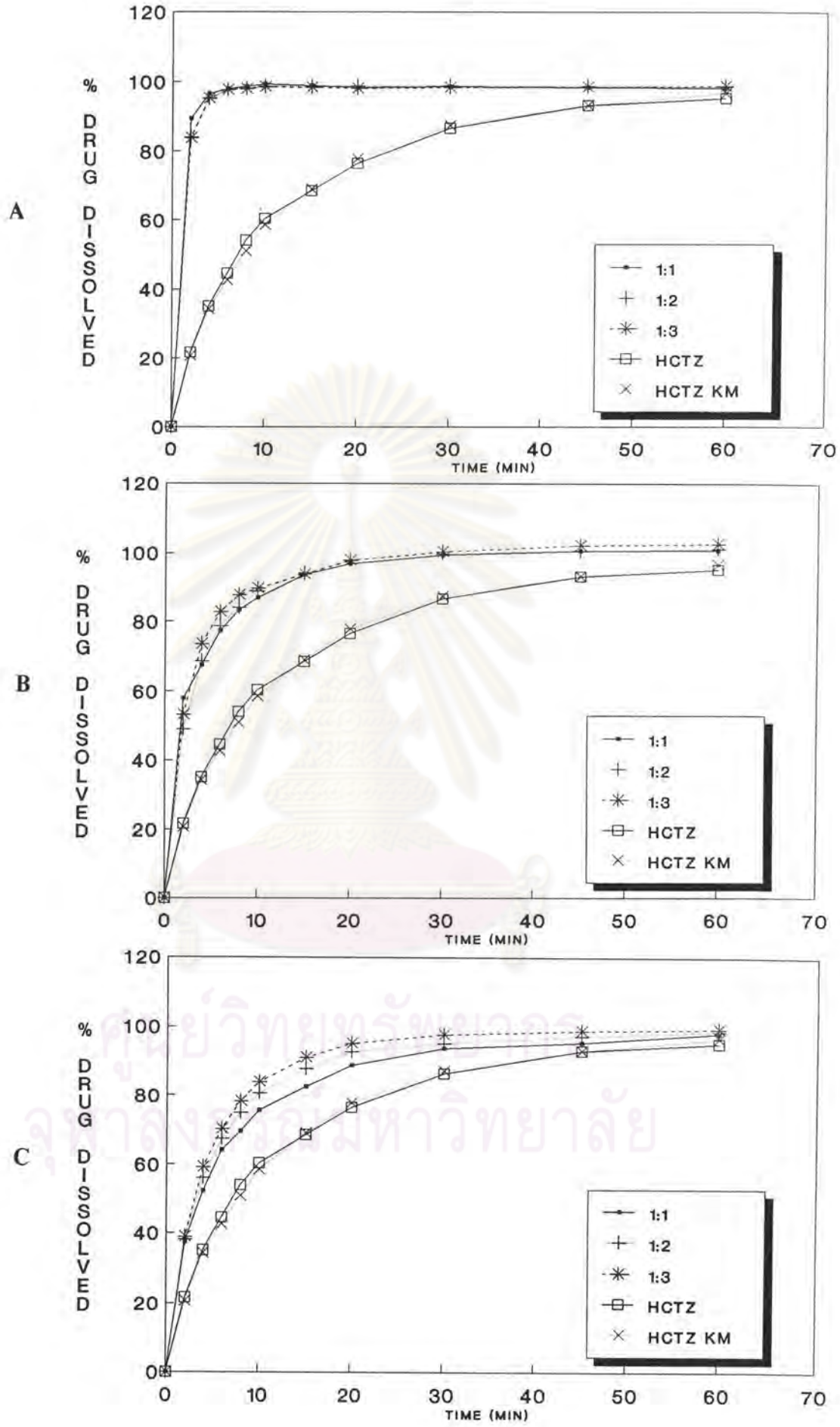

Figure 14 The dissolution profiles of HCTZ kneading mixture showing of three ratios (key : A-LMCS KM, B-PVP KM, C-PEG KM)

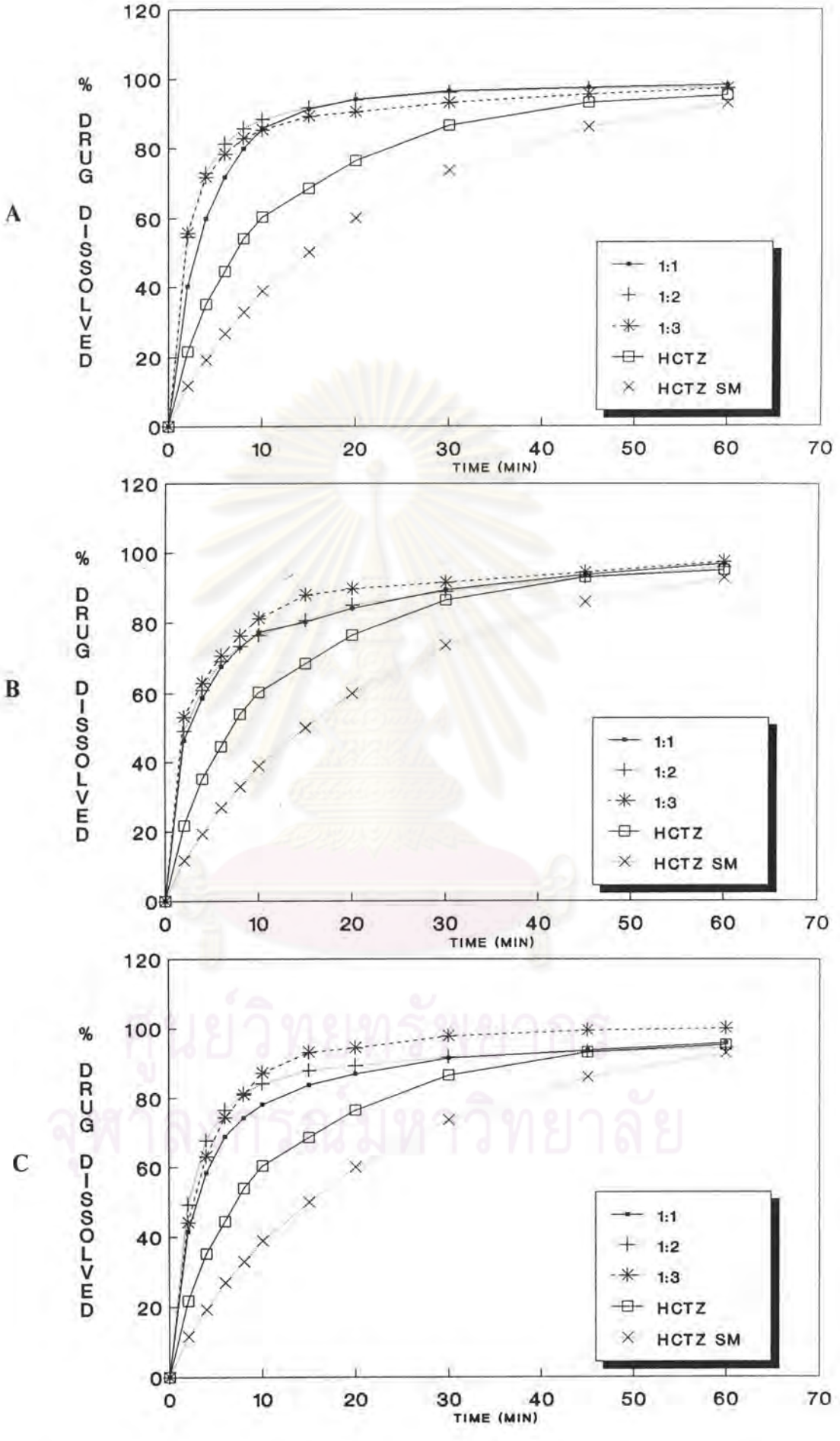

Figure 15 The dissolution profiles of HCTZ solvent deposition mixture showing of three ratios(key :A-CT SMD, B-CS SMD, C-CSU SMD)

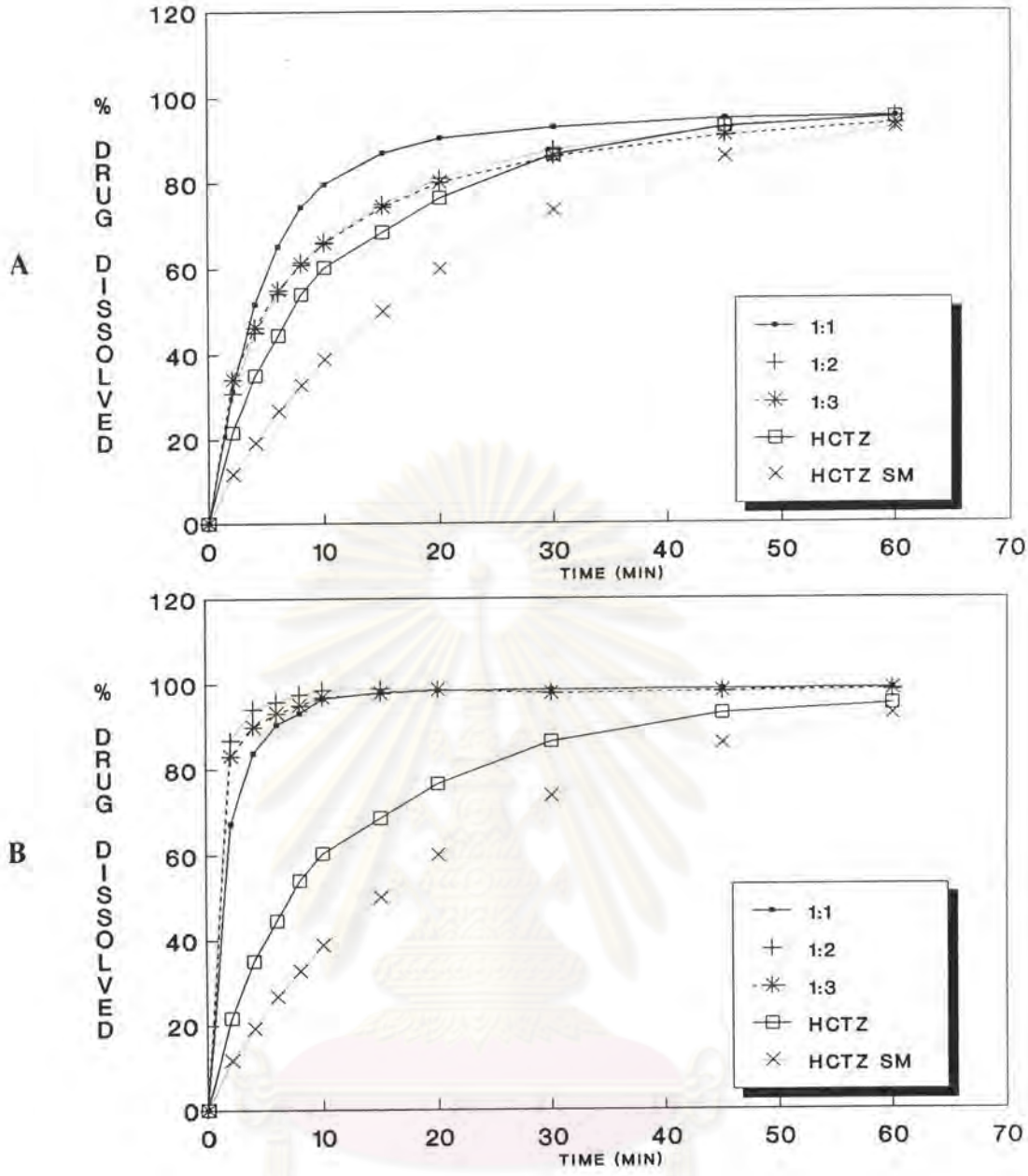

Figure 16 The dissolution profiles of HCTZ solvent and solvent deposition mixture showing of three ratios (key :A - LMCS SMD, B-LMCS SM)

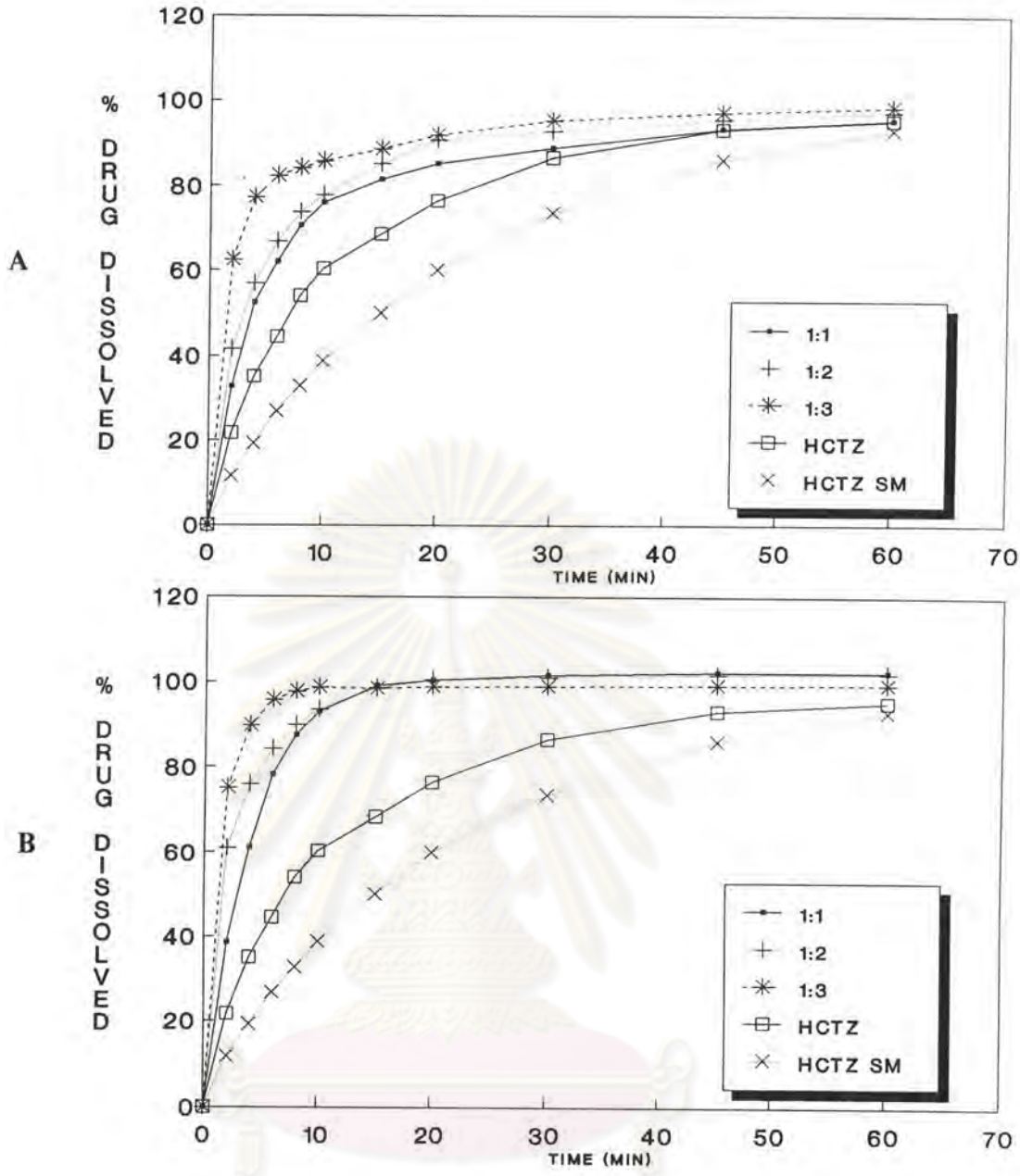

Figure 17 The dissolution profiles of HCTZ solvent mixture showing of three ratios (key:A-PVP SM,B-PEG SM)

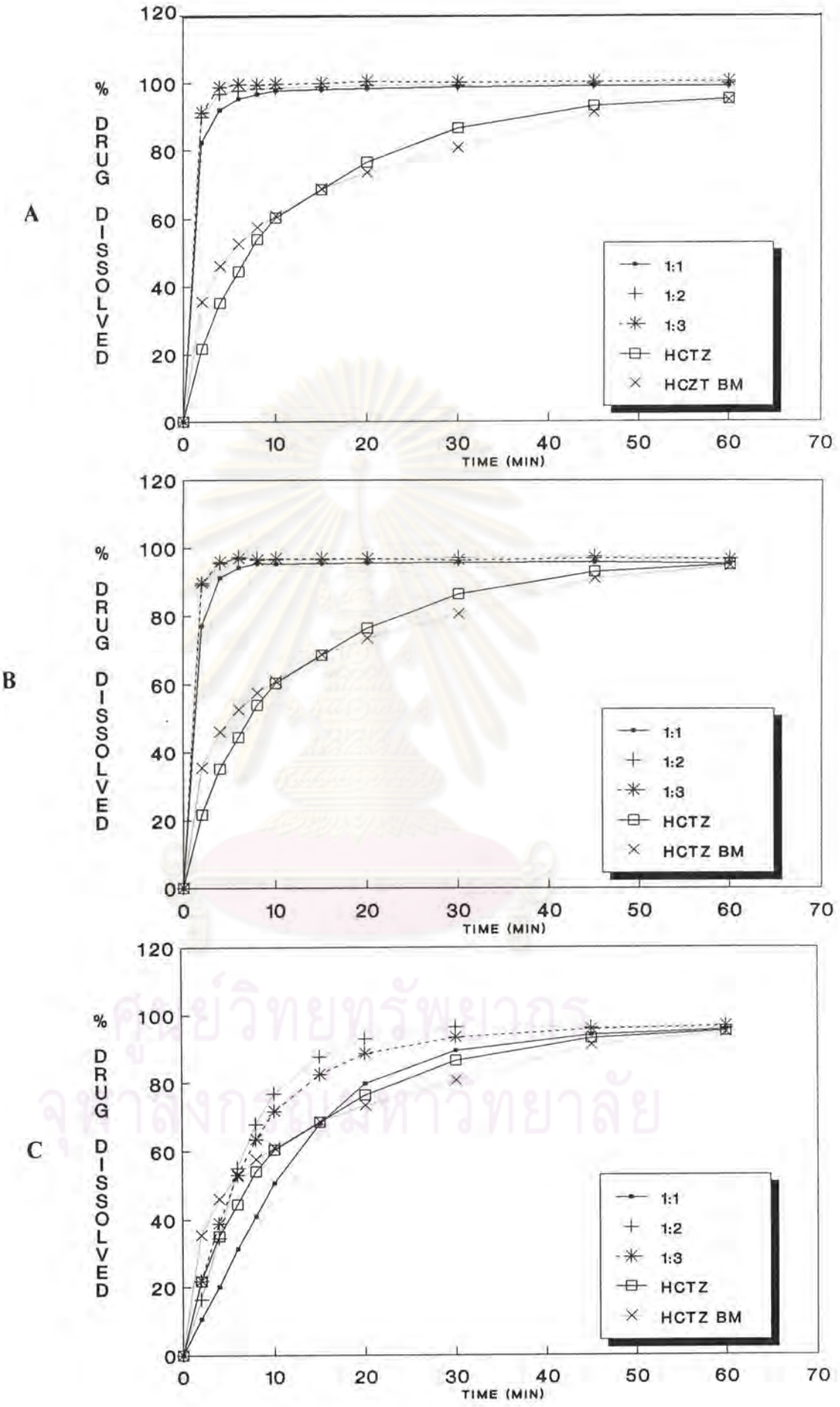

Figure 18 The dissolution profiles of HCTZ ball milling mixture showing of three ratios (key : A - CT BM, B- CS BM, C- CSU BM)

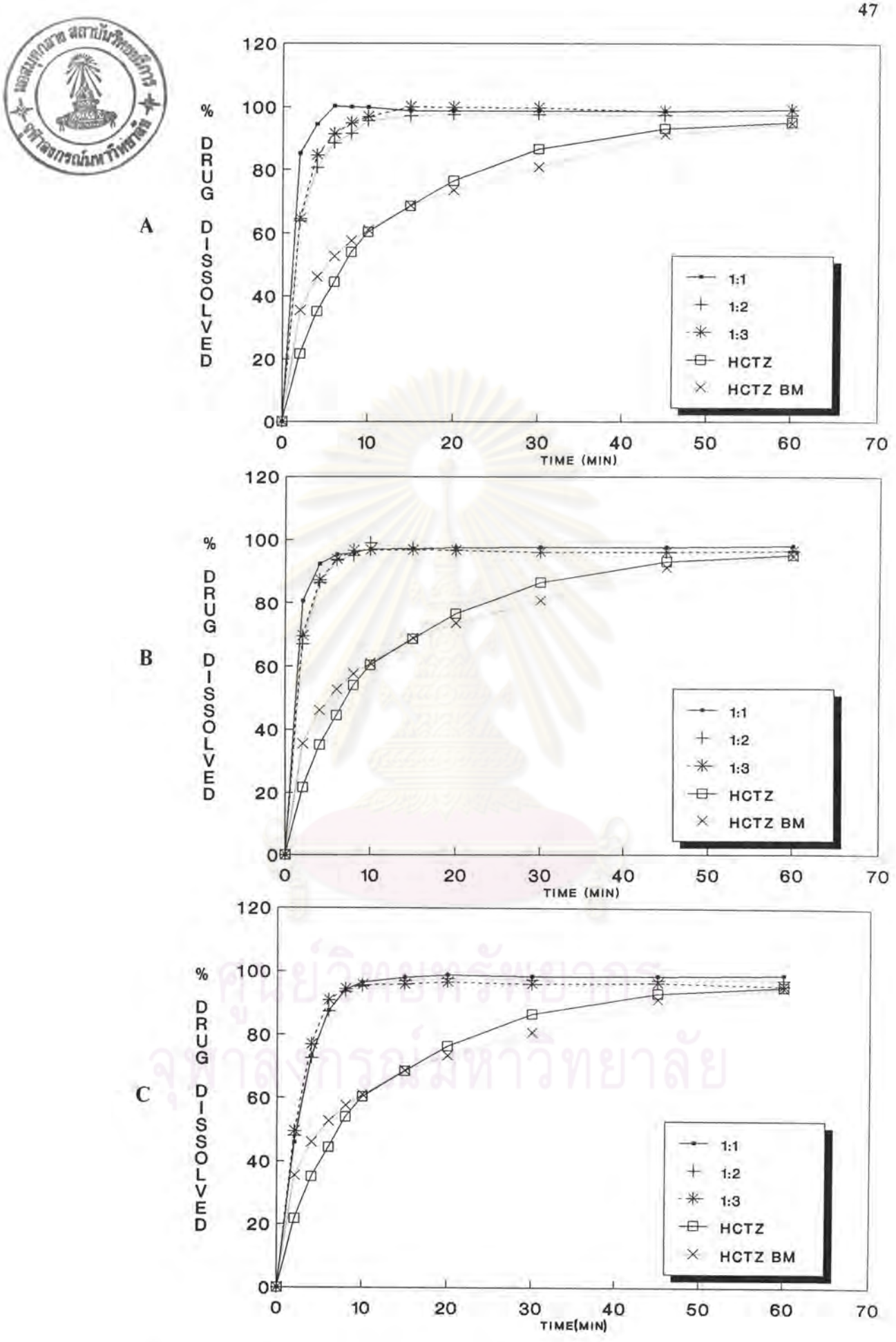

Figure 19 The dissolution profiles of HCTZ ball milling mixture showing of three ratios (key : A-LMCS BM-SW, B-LMCS BM-VB, C-PVP BM)

compared with HCTZ and HCTZ BM, except CSU BM which showed less drug dissolved in the early stage and then finally the same in the ratios of 1:2 and 1:3

In conclusion, the increment of carrier ratio ranging from 1 to 3 resulted in a slight increase in dissolution. Most mixtures evidently increased the dissolution when compared with pure and treated HCTZ.

Method Comparison

Four different methods of PM, KM, SM, and BM were employed to study their effects on drug dissolution enchancement. The dissolution profile allows the following remarks:

For CT, Figure 20, dispersion from ball milling method exhibited the fastest dissolution in the first 2 minutes. Following were the method of KM, SMD, PM and pure drug, respectively. Kneading method produce slightly higher dissolution profile, followed solvent deposition method in ratio of 1:1 and 1:3 but slightly lower at 1:2 ratio. All of the four methods showed higher dissolution than the pure drug.

For CS, Figure 21, the dissolution profile of the three ratios displayed the same pattern. Like chitin, ball milling method was the best method to obtain satisfactory dissolution. whereas the kneading method among the three ratios was considerably higher dissolution than the solvent deposition method. Compared with the three mentioned methods, physical mixture and pure HCTZ exhibited less drug dissolved.

For CSU, Figure 22, dispersions of any studied ratio showed different dissolution espectially when compared with CS. CSU BM was not the best method to obtain satisfactory dissolution as CS BM was. The highest dissolution was obtained from kneading method except for first 10 minutes which slightly lesser than those from CSU SMD and the greater. The order of increasing dissolution was as follows: KM > SMD > BM > PM > pure drug. CSU BM showed higher dissolution than CSU PM and pure drug except for first 15 minutes of 1:1 CSU BM which showed the lowest dissolution profile.

For LMCS, Figure 23, among prepared methods KM, SM and BM (SW and VB) were markedly greater in dissolution than PM and SMD method, the order of increasing dissolution was as follows: KM > SM > BM (SW, VB) > PM >SMD > pure drug. The best dissolution profile was obtained from kneading method. However the increment of dissolution from SM was nearly

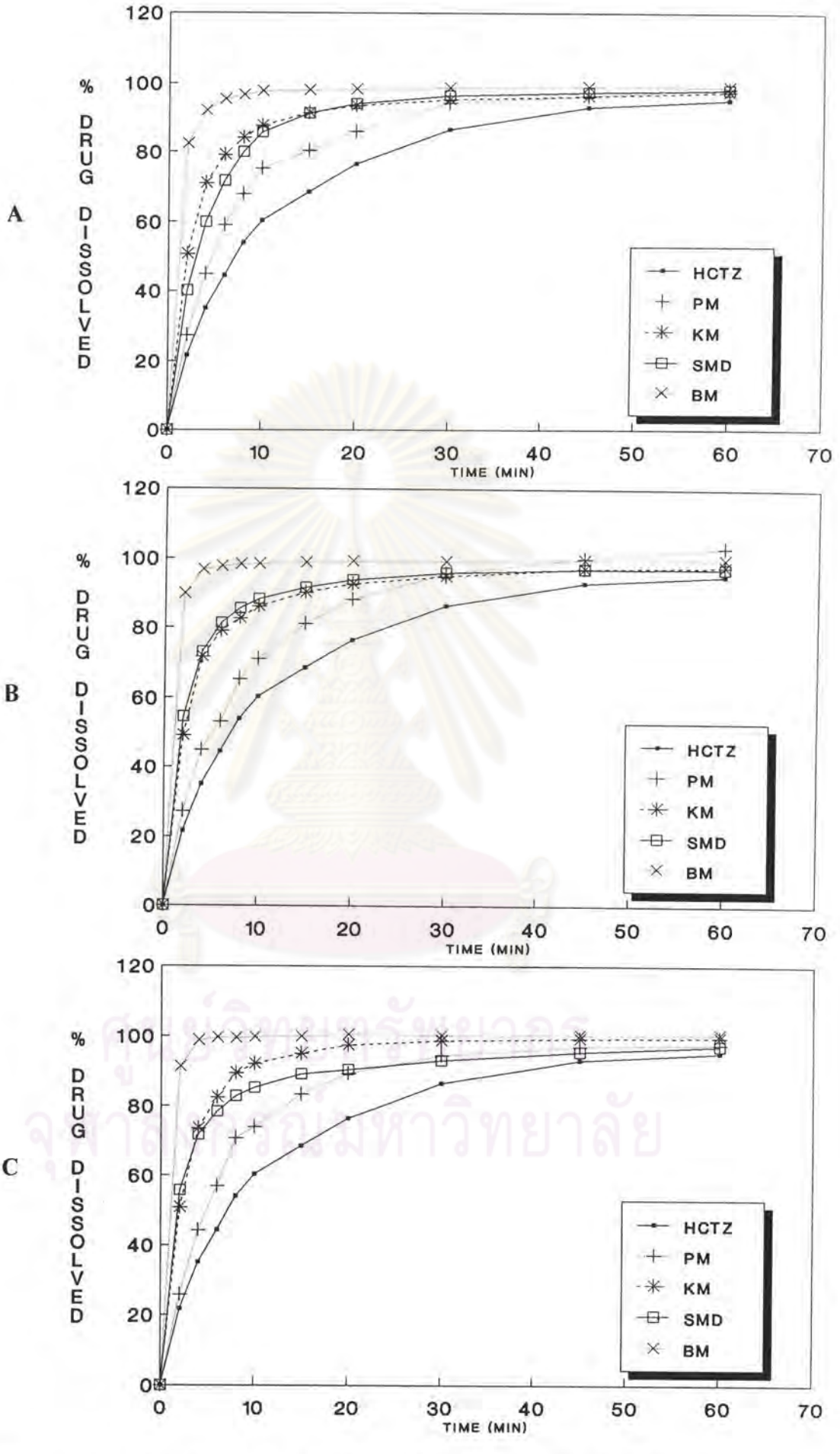

Figure 20 The dissolution profiles of HCTZ from HCTZ - CT mixture (key: A-1:1 CT, B-1:2 CT, C-1:3 CT)

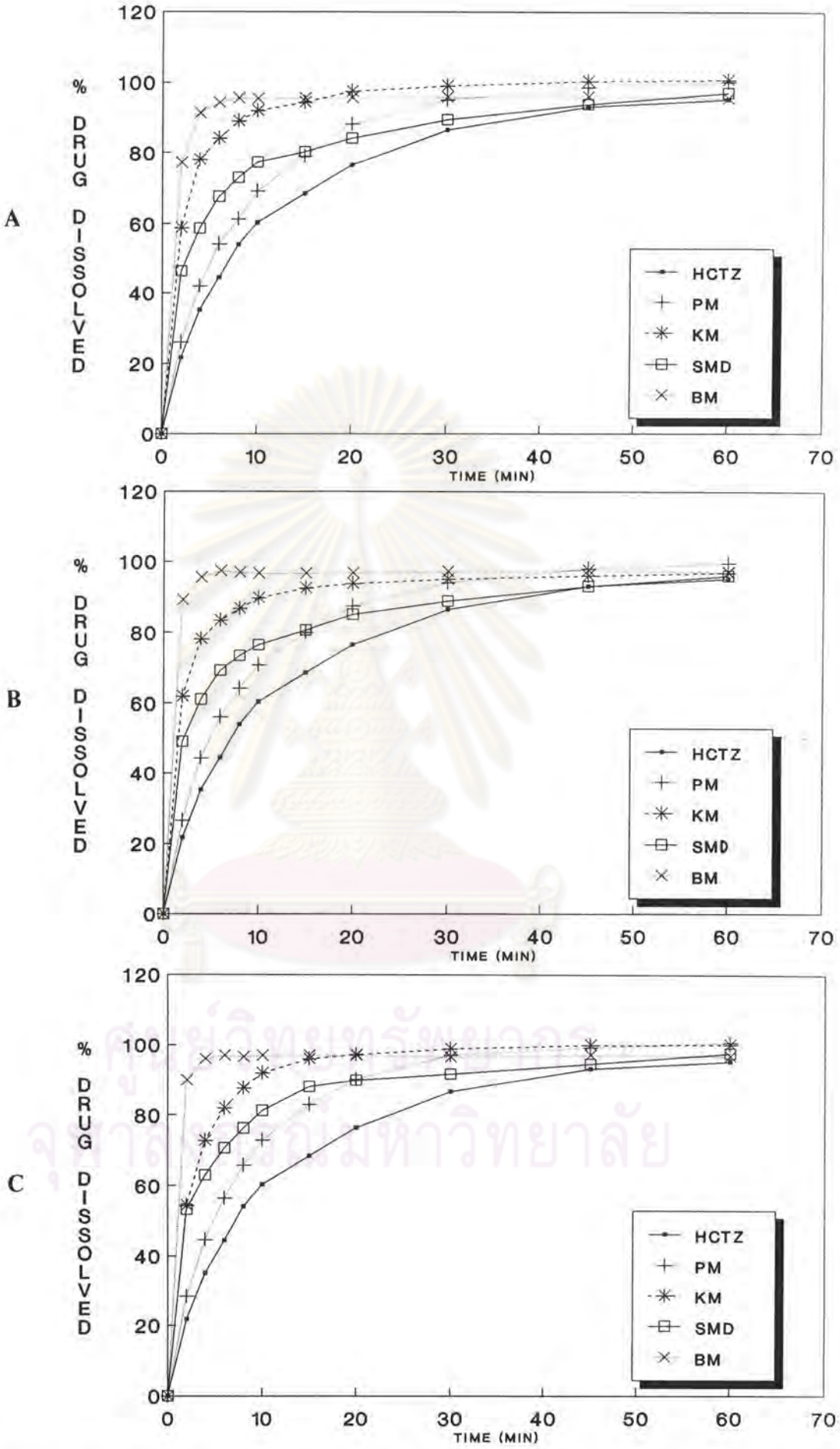

Figure 21 The dissolution profiles of HCTZ from HCTZ - CS mixture (key: A-1:1 CS, B-1:2 CS, C-1:3 CS)

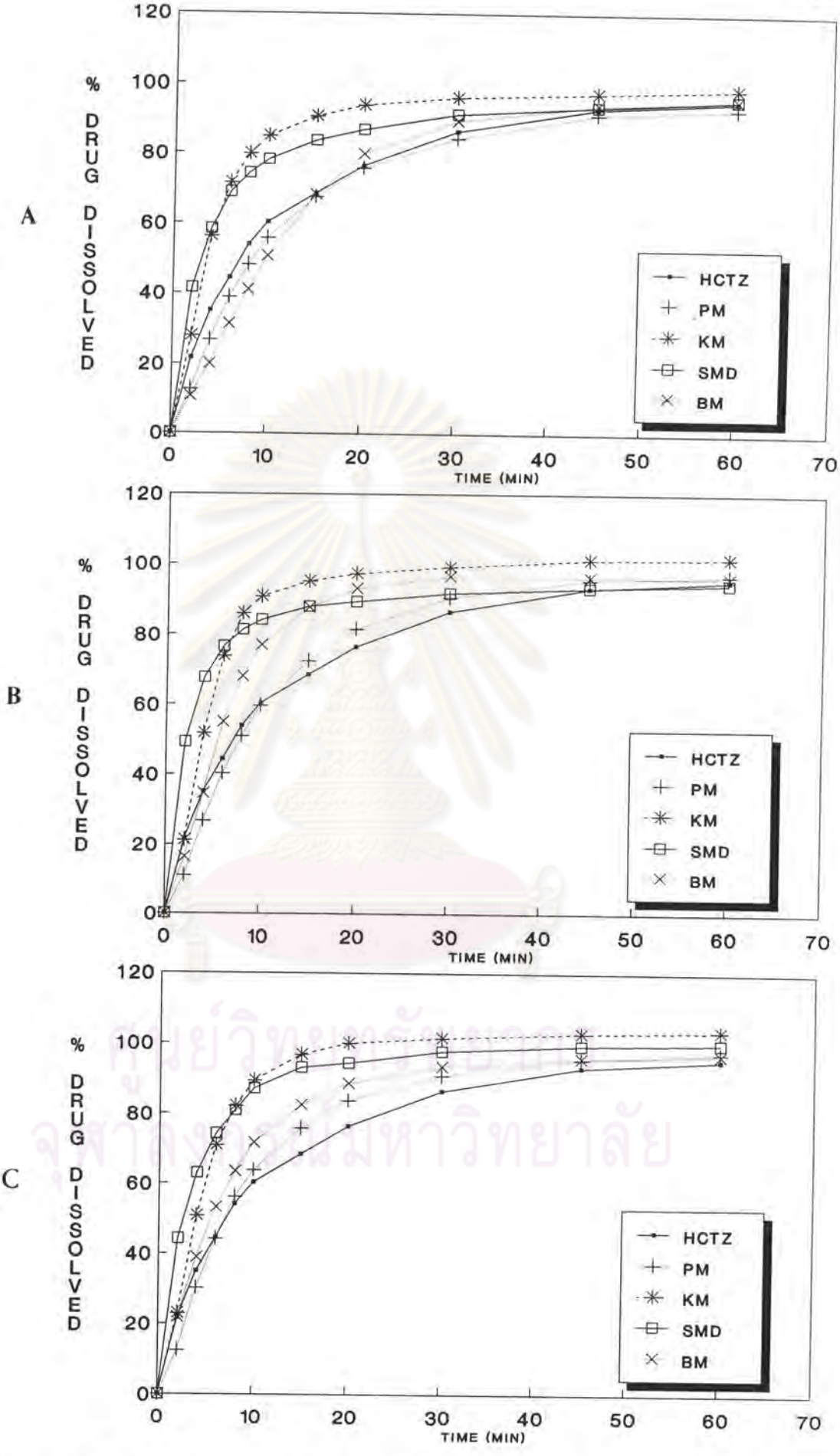

Figure 22 The dissolution profiles of HCTZ from HCTZ - CSU mixture (key:A- 1:1 CSU, B-1:2 CSU, C-1:3 CSU)

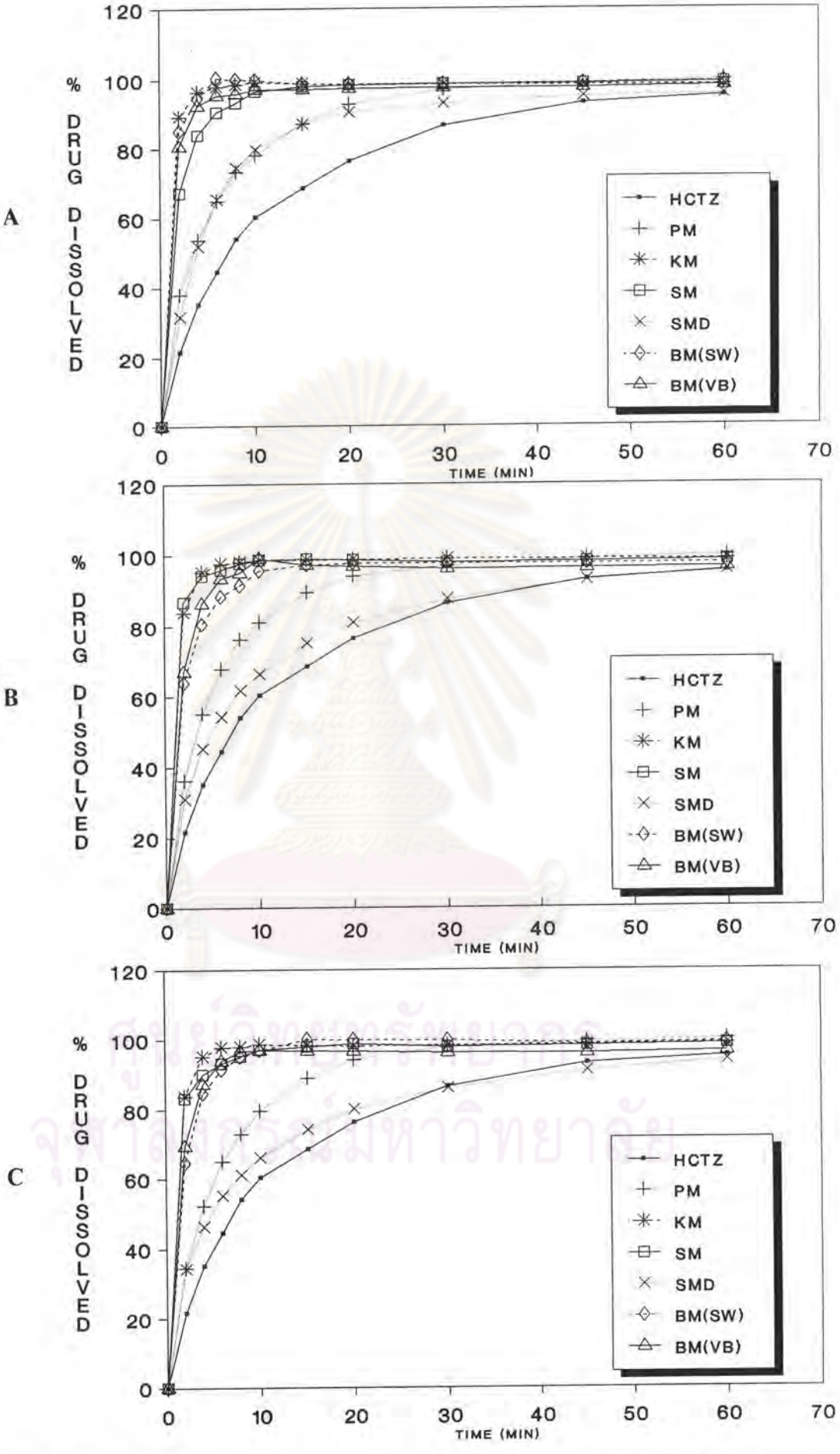

Figure 23 The dissolution profiles of HCTZ form HCTZ-LMCS mixture (key : A-1:1 LMCS, B-1:2 LMCS, C-1:3 LMCS)

equal to KM method, espectially at 1:2 and 1:3 LMCS SM. When comparing between SM and SMD, both methods showed a remarkable difference in dissolution profile, that of SM were obviously higher than SMD. In contrast, LMCS SMD showed the lowest dissolution compare with other methods. The dissolution profile from milling method was markedly increased next to SM method, except for ratio of 1:1 BM which were slightly higher than 1:1 SM. BM(VB) dispersions showed slightly higher dissolution than BM(SW) at ratio of 1:2 and 1:3. However, both VB and SW profiles were nearly equal. In addition, the dissolution from physical method also increased, and was higher than those of SMD and pure drug.

For PVP, Figure 24, the highest dissolution was obtained from ball milling method, followed by kneading solvent and physical method. All of three ratios were in the same pattern except for 1:3 PVP SM which exhibited higher dissolution than 1:3 PVP KM in the first 5 minutes.

For PEG, Figure 25, the highest dissolution was obtained from solvent method, followed by kneading and physical method, respectively. All of three ratios showed the same dissolution pattern.

In conclusion, ball-milled method showed a remarkable increase in dissolution for all carriers except CSU. Kneading method and solvent method also produced dominantly higher drug dissolved in some carriers such as LMCS in both methods, while PEG in the solvent method. In short, the three mentioned methods exhibited higher percentage of drug dissolved than pure drug and physical mixtures.

Carrier Comparison

In this study, six carriers with different characteristics were chosen to compare the enhancement in dissolution. Variation in released profile was remarkably observed in each carrier.

Comparison in physical method, Fig 26 showed that dissolution of 1:1 ratio was slightly different in each carrier. LMCS exhibited the highest followed by CT, CS, PEG and PVP respectively. All carriers produced higher dissolution than HCTZ or HCTZ PM except CSU and PVP. Dissolution of 1:2 was also the same order but PEG showed slightly higher dissolution than CS. In addition, ratio of 1:3 was as the same as ratio 1:2 except CSU which dissolution was higher than that of HCTZ.

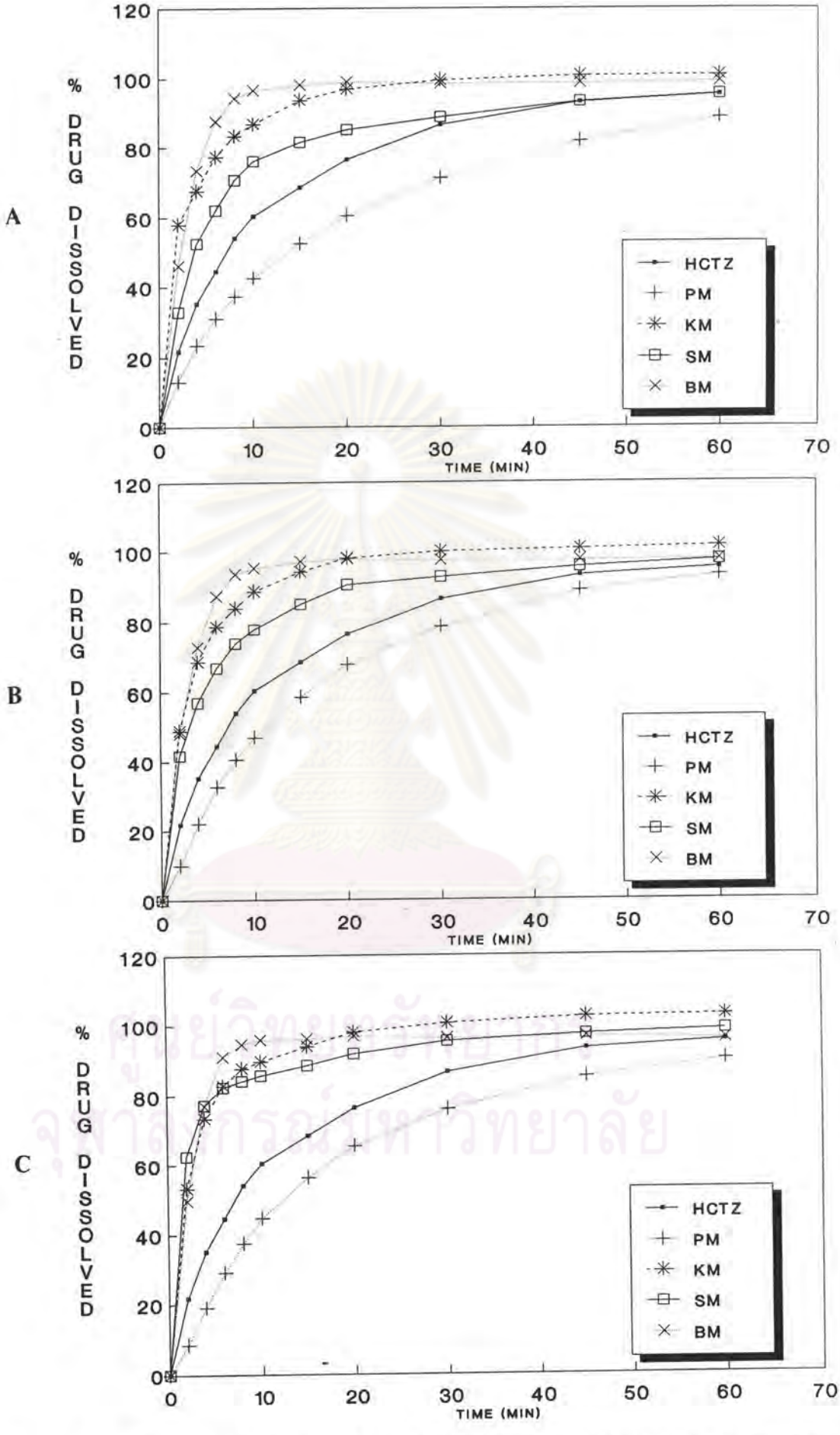

Figure 24 The dissolution profiles of HCTZ from HCTZ - PVP mixture (key : A-1:1 PVP, B-1:2 PVP, C-1:3 PVP)

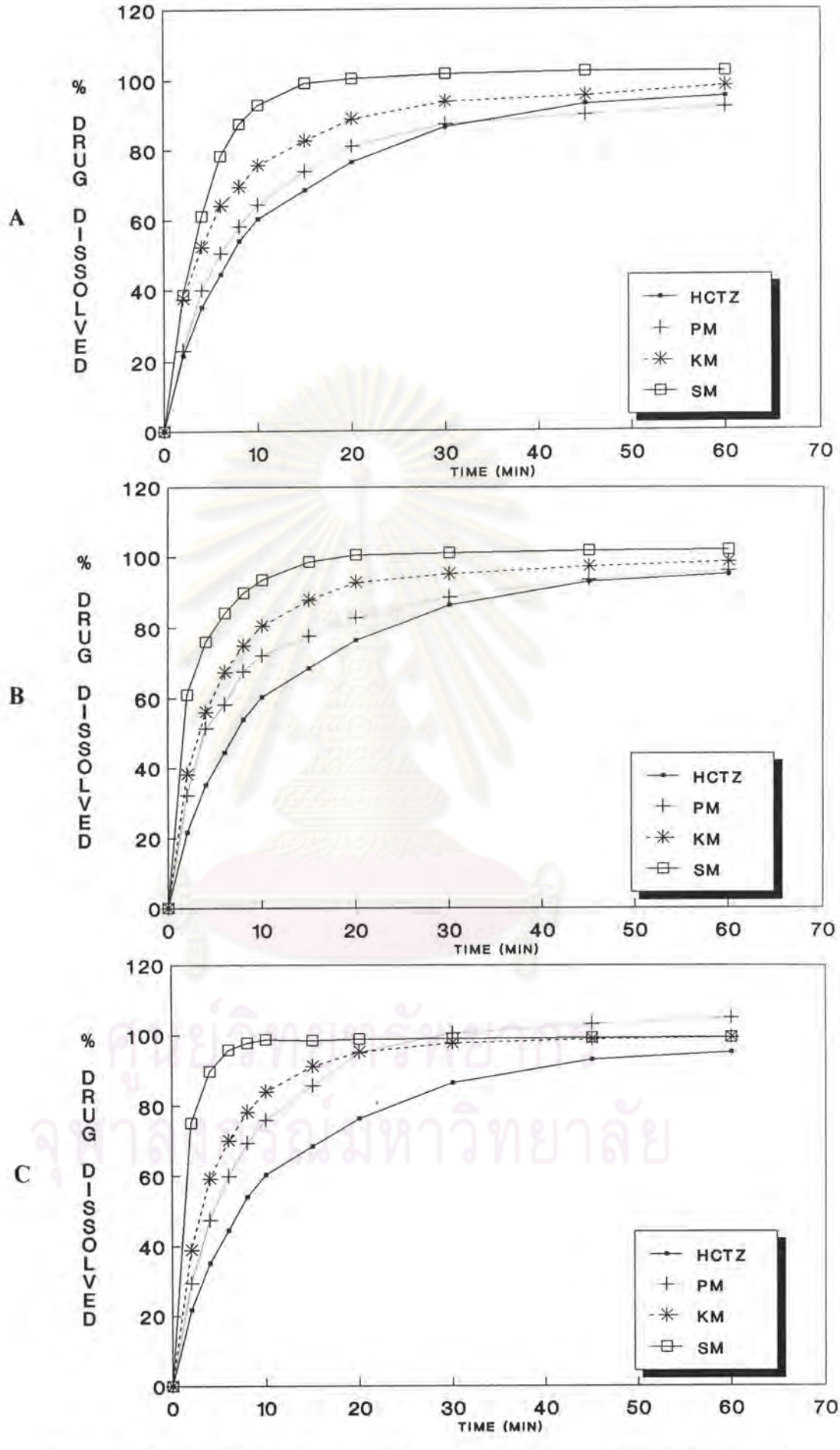

Figure 25 The dissolution profiles of HCTZ form HCTZ-PEG mixture (key : A-1:1 PEG, B-1:2 PEG, C-1:3 PEG)

A

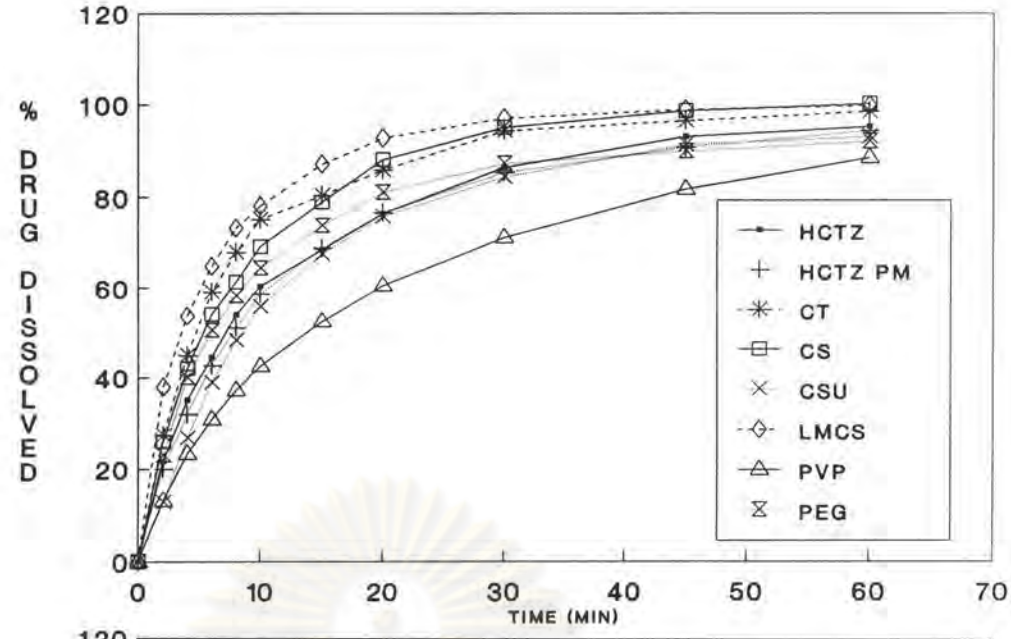

B

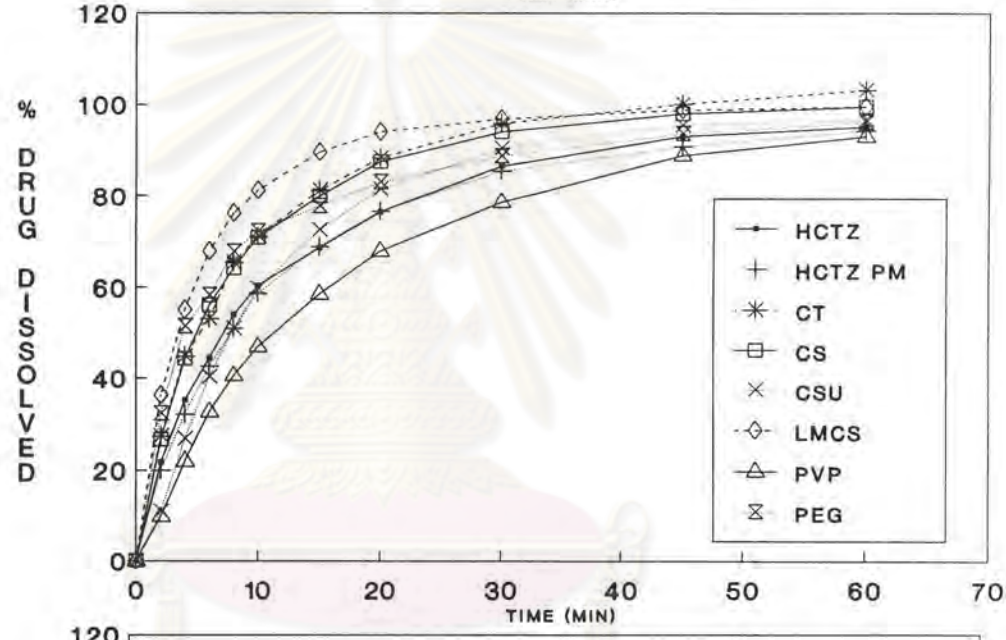

C

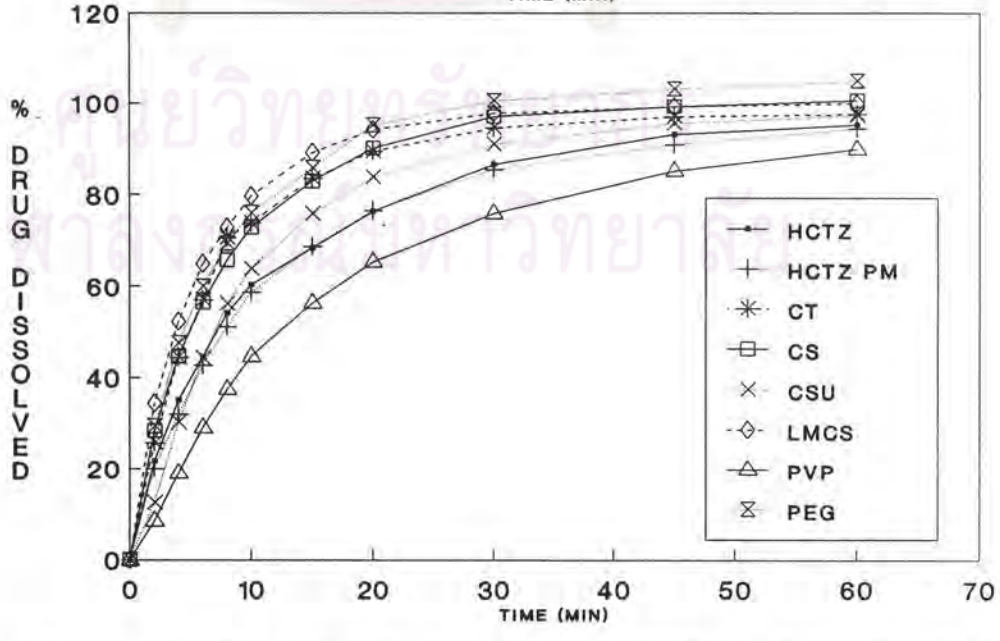

Figure 26 The dissolution profiles of HCTZ by physical method (key : A - 1:1 PM, B -1:2 PM, C-1:3 PM)

In the case of kneading method, Fig 27, all ratios showed the same dissolution pattern. LMCS exhibited tremendously fastest dissolution than CS, CT, PVP, CSU and PEG respectively. All carriers also displayed higher dissolution than HCTZ KM and pure drug.

In the case of solvent method, Fig 28, dissolution of ratio 1:1 was different in each carriers. The highest was from LMCS (SM), followed with PEG, CT, LMCS(SMD), CSU, PVP and CS respectively. The ratio of 1:2 and 1:3 showed the same order except LMCS SMD showed lower dissolution than PVP. Moreover, in the 1:3 ratio, PVP showed higher dissolution than CT.

Finally, in ball milling method, Fig 29, dissolution profile was only slightly different in each carrier except CSU. Ratio 1:1, the order of increasing dissolution was LMCS(SW) > CT > LMCS(VB) > CS > PVP. Ratio 1:2, the increment was in the order CT > CS > LMCS (VB, SW) > PVP. Similarly, ratio 1:3 showed the same pattern as ratio 1:2 in dissolution profile. All carriers of CT, CS, LMCS, PVP showed more percentage of HCTZ dissolved than CSU, HCTZ BM and HCTZ respectively.

In summary, LMCS seemed to be the best carrier with highest percentage of HCTZ dissolved in several methods. CT and CS showed the best dissolution in ball milling method, and so did PEG in solvent method.

Tablet Evaluation

For tabletting, only 1:1 ratio of dispersion mixtures were selected due to the suitable quantity of carrier. The higher the amount of carrier, the higher the size and the cost of tablets. Dispersion mixtures of promising dissolution, CSU KM, LMCS SM, PEG SM, CT BM, CS BM, LMCS BM(SW&VB) and PVP BM were made to tablets. The USP XXII requirement for HCTZ tablets is that "no less than 60% of the labeled amount of $C_7H_8CLN_3O_4S_2$ is dissolved in 60 minutes using apparatus I, at 100 rpm, in 900 ml of 0.1 N HCL".

The prepared tablets were evaluated for mean weight, disintegration time, hardness, and dissolution studies, compared with two commercial HCTZ tablets (brand A, brand B). The results were summarized in Table 3 and Figure 30.

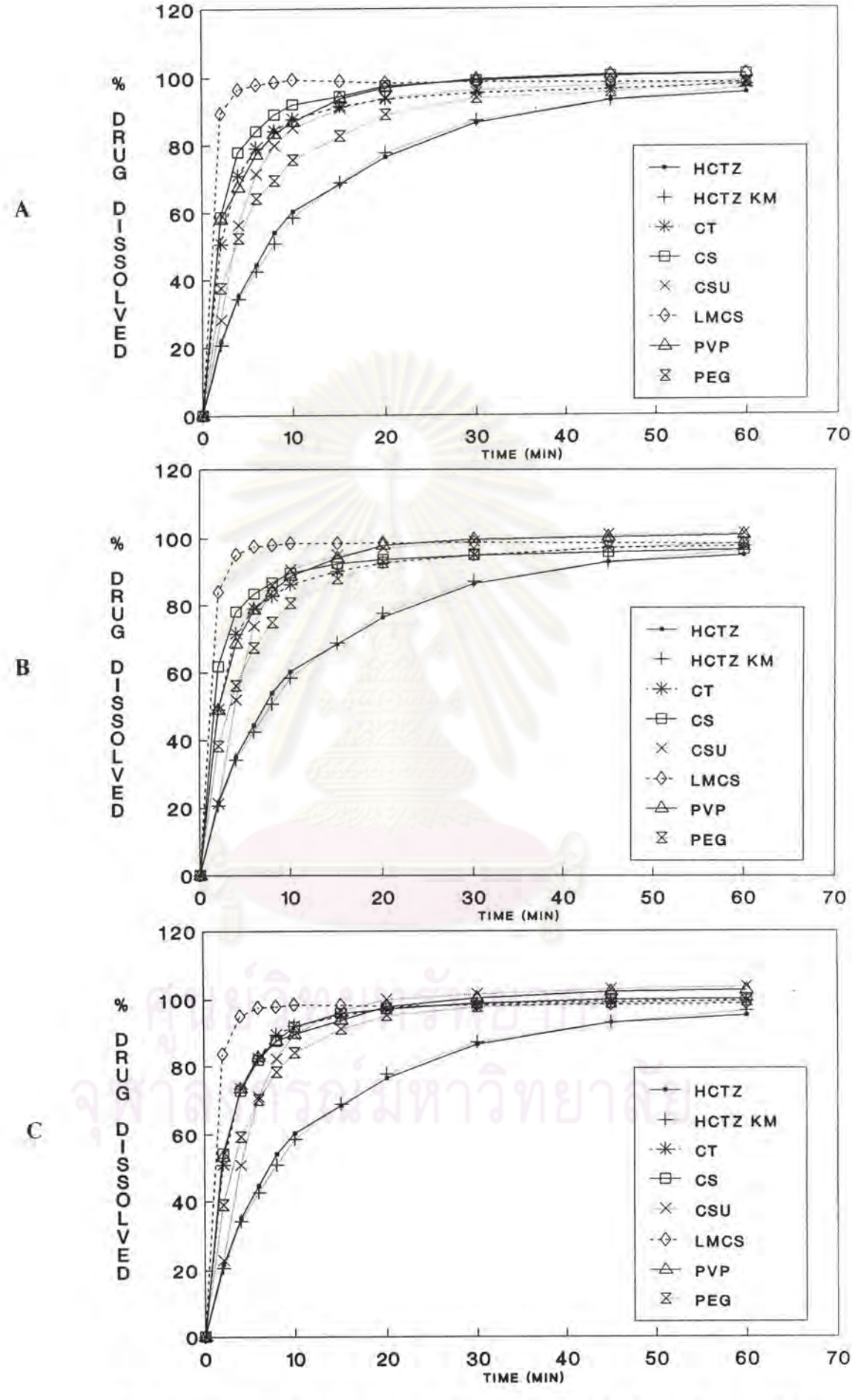

Figure 27 The dissolution profiles of HCTZ by kneading method (key : A-1:1 KM, B-1:2 KM, C-1:3 KM)

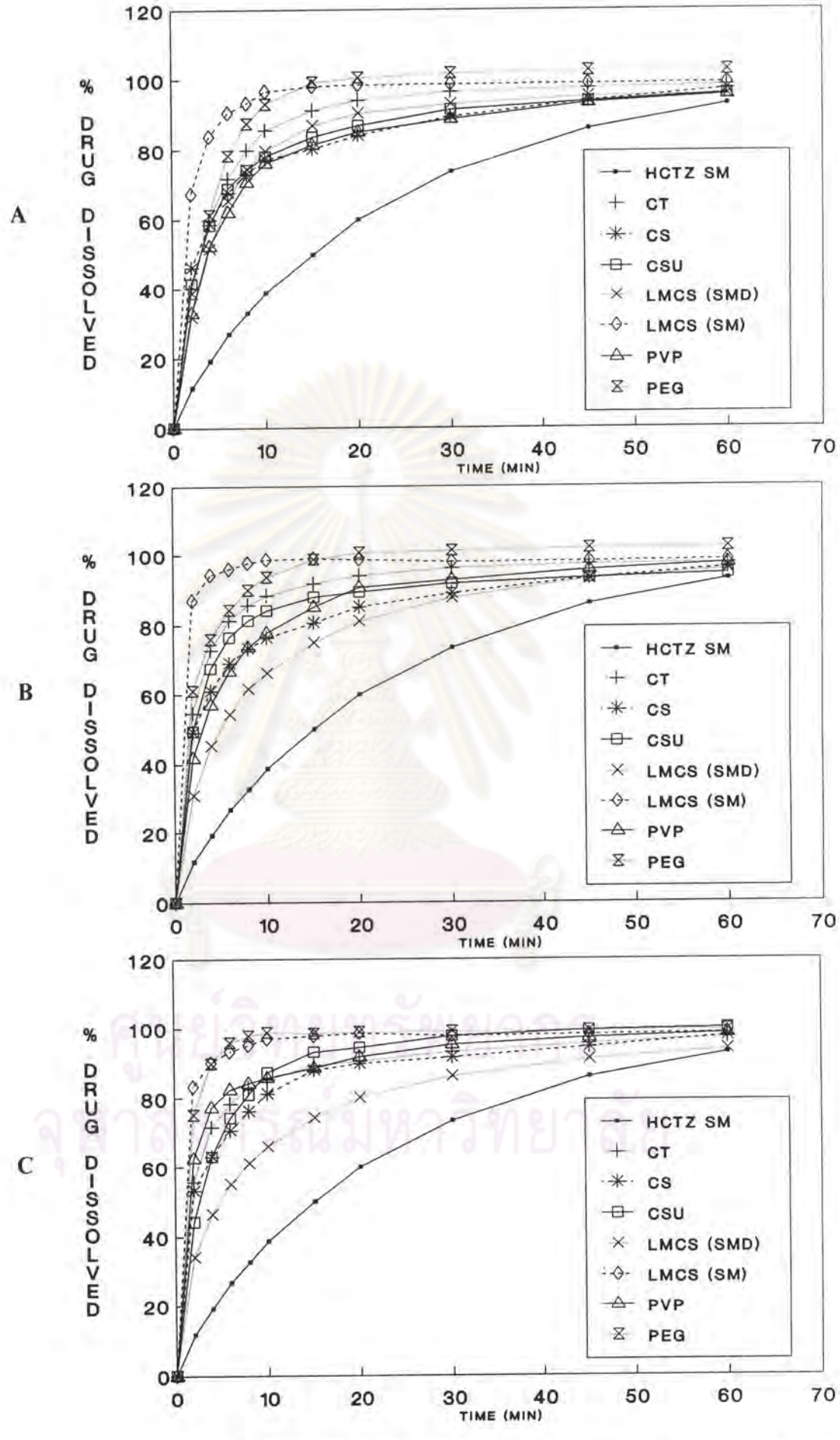

Figure 28 The dissolution profiles of HCTZ by solvent method (key : A-1:1 SM, B-1:2 SM, C-1:3 SM)

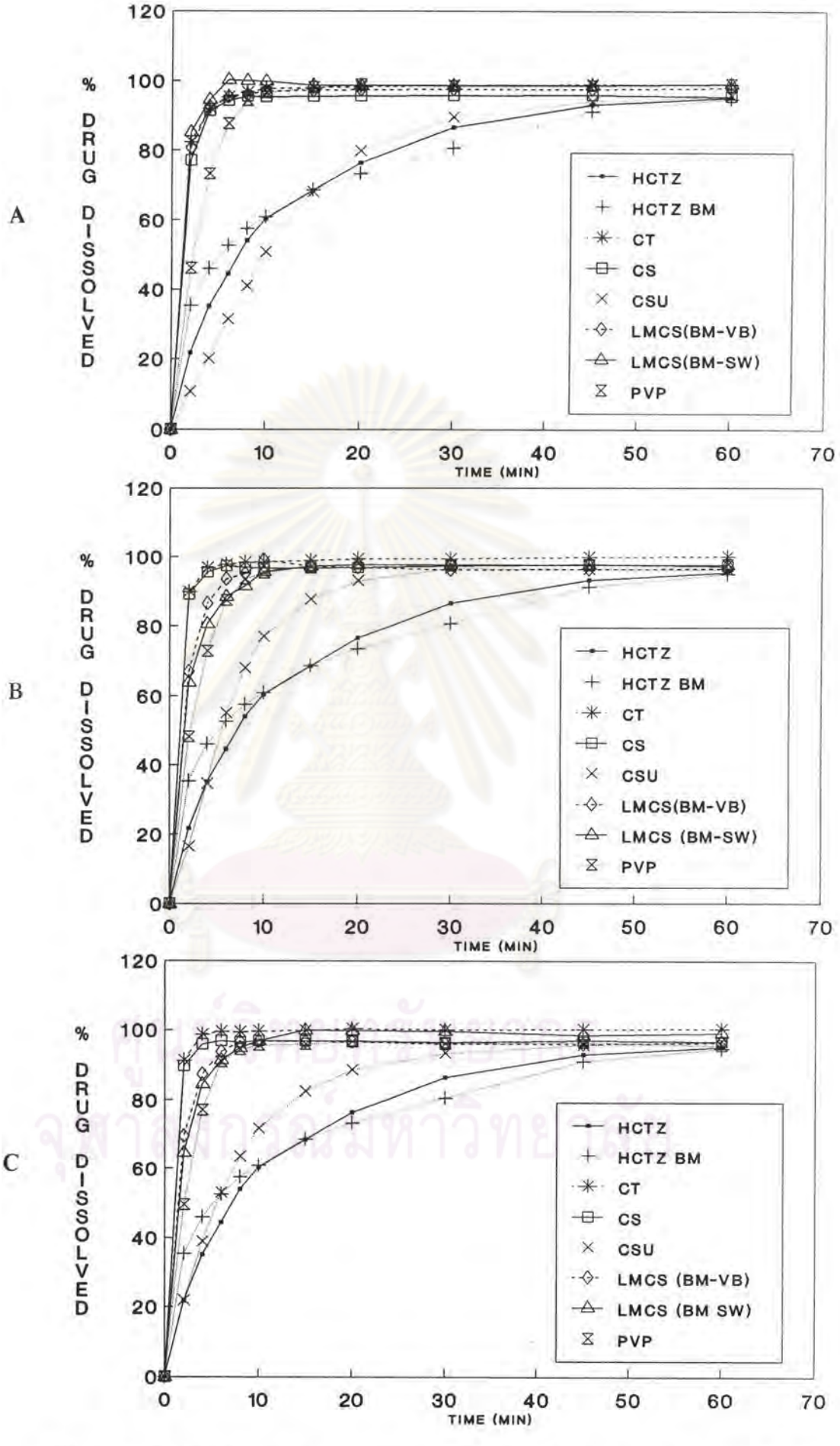

Figure 29 The dissolution profiles of HCTZ by ball milling method (key : A-1:1 BM, B-1:2 BM, C-1:3 BM)

Mean Weight

The weight and the average values of ten prepared HCTZ tablets and commercial products are presented in Appendix III (Table 28). The mean weight of prepared tablets ranged from 214.4 mg to 217.7 mg, while those two commercial tablets were 210.8 mg and 209.3 mg.

Disintegration Time

The disintegration time and the average values of each prepared HCTZ tablets and commercial products are presented in Appendix III (Table 29). It was a remarkable observation among those produced tablets. Disintegration time was increased in the order of CT BM < CS BM < brand A < LMCS SM < PEG SM < LMCS BM(SW, VB) < PVP BM < brand B , and was in the range of less than 1 minute to over 14 minutes. Only PVP BM and commercial brand B possessed the longest time for disintegration.

Hardness

The hardness and the average values of each prepared HCTZ tablets and commercial products are presented in Appendix III (Table 30). In prepared tablets, the hardness was in the range of 4.5-8 kp except blank and PVP BM which had the hardness about 2.4 kp and over 10 kp.Most prepared tablets had the hardness nearly to the hardness of commercial tablets.

Dissolution studies of tablet

The dissolution profiles and data of prepared tablets and commercial ones are presented in Figure 30 and Appendix III (Table 24-27).

Comparison of $T_{60\%}$ among those produced tablets and those of commercial tablets which was the time that was taken to dissolve 60% of HCTZ. This amount of time could be measured by extrapolating the 60% of HCTZ to the dissolution-time curve. The results (in Table 4) showed that the in creasing of $T_{60\%}$ was in the order of : CT BM < CS BM < LMCS SM < LMCS KM < PEG SM < LMCS BM (SW, VB) < brand A < PVP BM < brand B < CSU KM with the time were 2.5, 3.12, 4.37, 4.68, 4.96, 5.62, 24.4, 25.31, 30 and over 60 minutes, respectively.

Almost all prepared tablets exhibited distinguished enhancement of dissolution than the blank tablet and two commercial tablets, except PVP BM and CSU KM tablets. The dissolution results from these studies indicate that the produced tablets comply with the USP, except CSU KM tablet.

Table 3 The physical properties of prepared–HCTZ tablets compared with two commercial–HCTZ tablets

Tablet Formula	Physical Properties of Tablet					
	Weight (mg)		Disintegration time (min)		Hardness (Kp)	
	avg (n = 10)	S.D.	avg (n = 6)	S.D.	avg (n >= 3)	S.D.
Prepared Tablet (1:1)						
Blank	214.80	0.45	0.19	0.01	2.40	0.45
CSU KM	217.70	0.44	0.16	0.01	5.40	0.16
LMCS KM	216.60	0.31	2.17	0.10	5.40	0.65
LMCS SM	215.40	0.55	1.82	0.29	4.67	0.19
PEG SM	215.80	0.32	4.29	0.61	6.67	0.94
CT BM	215.80	0.38	0.09	0.02	6.10	0.22
CS BM	215.30	0.62	0.09	0.02	7.07	0.34
LMCS BM (SW)	215.70	0.42	4.51	0.25	7.60	0.73
LMCS BM (VB)	214.40	2.66	4.63	0.33	8.07	1.03
PVP BM	217.70	0.28	14.04	1.27	10.93	0.62
Commercial Tablet						
Brand A	210.80	2.87	2.14	0.09	5.63	0.70
Brand B	209.30	3.94	14.09	0.96	5.20	0.82

A

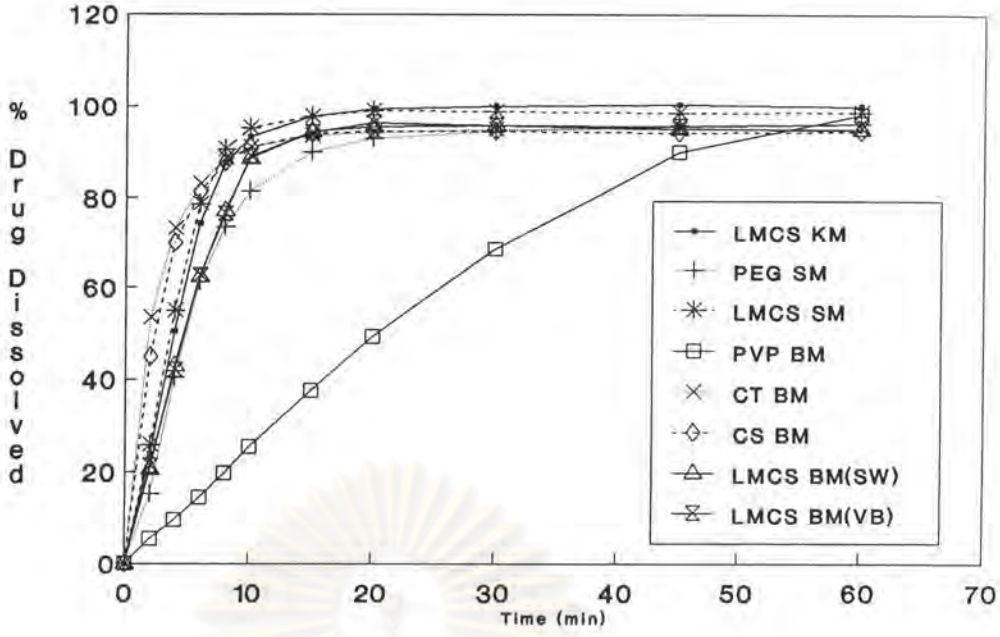

B

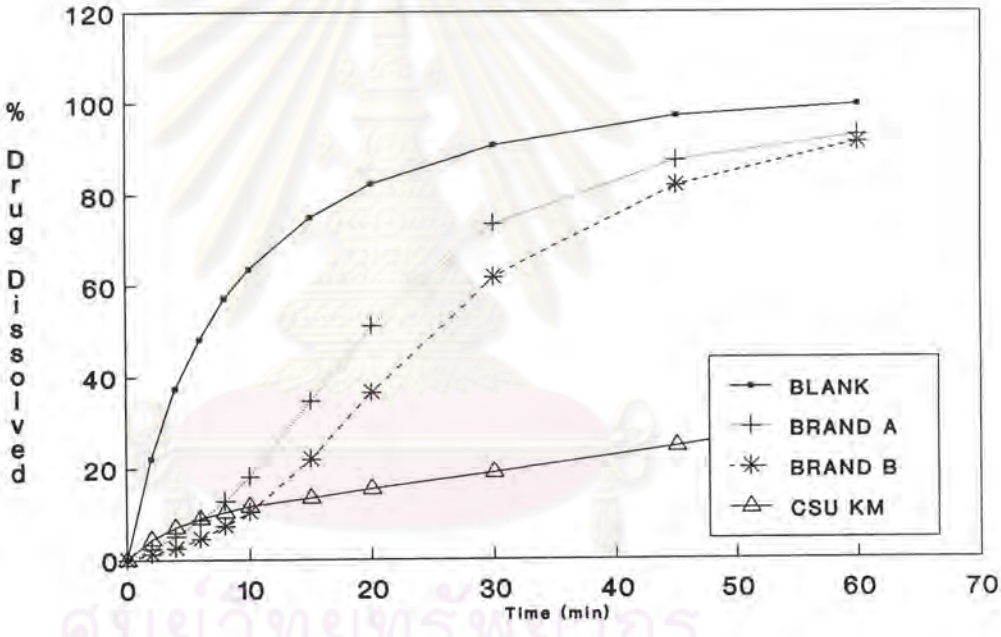

Figure 30 The dissolution profiles of HCTZ prepared and commercial tablets (key:A-HCTZ prepared tablets, B-blank, prepared and commercial tablets)

Table 4 The time 60% of HCTZ from all tablets dissolution.

THE TIME 60%	
Sample	$t_{60\%}$ (min, sec)
Prepared Tablet (1:1)	
Blank	9 : 34
CSU KM	>60
LMCS KM	4: 68
LMCS SM	4 :37
PEG SM	4 : 96
CT BM	2 : 50
CS BM	3 : 12
LMCS BM SW	5 : 62
LMCS BM VB	5 : 62
PVP BM	25 : 31
Commercial Tablet	
Brand A	24 : 4
Brand B	30 :0

Physicochemical Properties Studies

1. Particle Size Appearance

Scanning electron micrographs of HCTZ, carriers and all types of dispersion at the ratio 1:3 are illustrated in Figures 31-43 for observations of particle appearance at different magnification factors, low at x50, high at x500 or x2000.

1.1 HCTZ

Figures 31-32 are illustrations of pure HCTZ. HTCZ (A and B in Fig 31) was composed of flaky shape in various sizes ranging from 10 to >500 micron and had a rather smooth surface. HCTZ PM (C and D in Fig 31) showed the same appearance of HCTZ as before being treated. While most particles of HCTZ KM (E and F in Fig 31) were of irregular shapes and narrower size range of 10-150 micron, some of them agglomerated in large size with the irregular surface. Moreover, after being treated with appropriate solvents, HCTZ appearance changed into a new form (A and B in Fig 32) like cluster of cuboid with some small particles adhered on the smooth surface. The length of long cuboid was about 10-200 micron. Photomicrographs of treated HCTZ by ball-milling are shown in Figure 32 (C, D, E). Agglomerate of very fine particles of <10 micron was found and its particles had diameter ranging from 10 to 50 micron.

1.2 Carriers

By scanning electron microscope examination, six carriers were observed to identify its characteristic as shown in Figure 33-34.

The microscopic appearance of chitin was shown in Figure 33 (A and B). Its shape was ellipse-plate like and crinkly of rim with rather smooth surface. The length of chitin was about 300-500 microns.By means of comparison, Chitosan and Chitosan from Unicord, as portrayed in Figure 33 (C, D, E, F), disclosed that their characteristics was the same as chitin. Conversely, the Figure 34(A and B) explained low molecular weight chitosan which was different in characteristic from chitin or chitosan. Their smaller particle size and riddle of the surface distinguished from both chitin and chitosan.

The photomicrographs of PVP (C and D in Fig 34) mainly consisted of small and smooth surface of spherical particles with diameter of

A

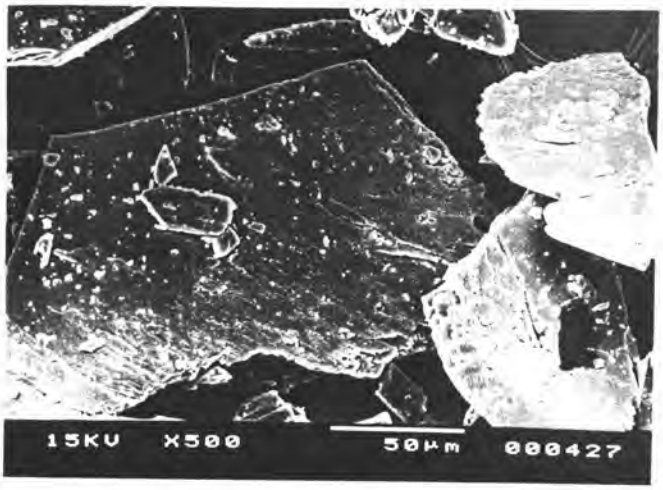

B

C

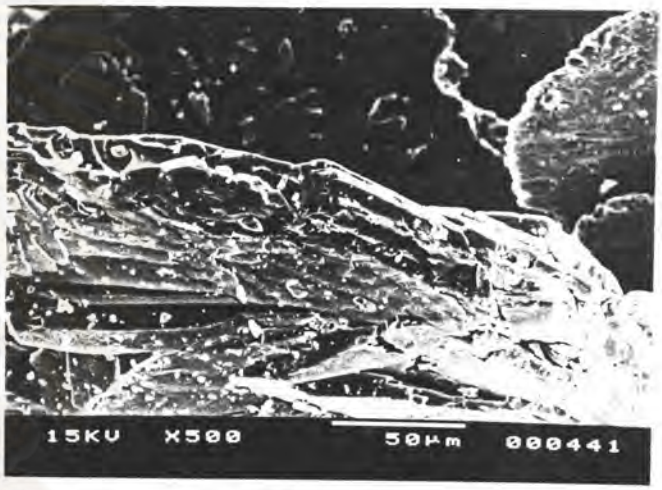

D

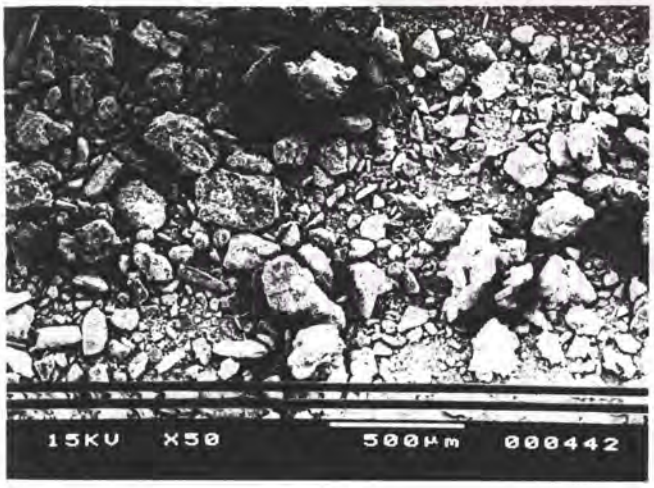

E

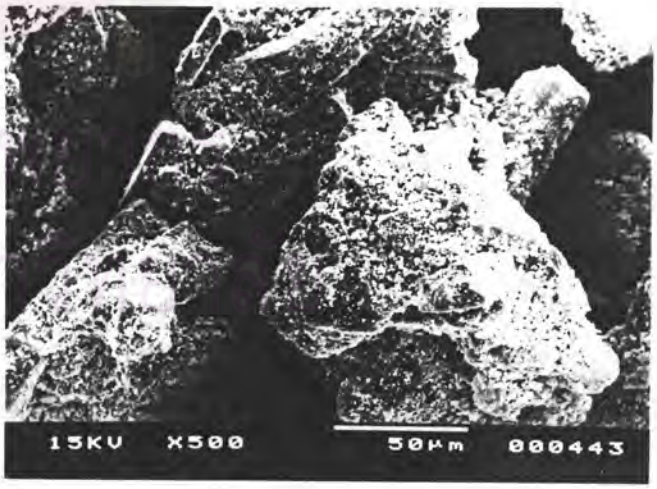

F

Figure 31 The photomicrographs of HCTZ and treated HCTZ
(key : A-HCTZ x 50, B-HCTZ x 500, C-HCTZ PM x 50
D-HCTZ PM x 500, E-HCTZ KM x 50,F-HCTZ KM x 500)

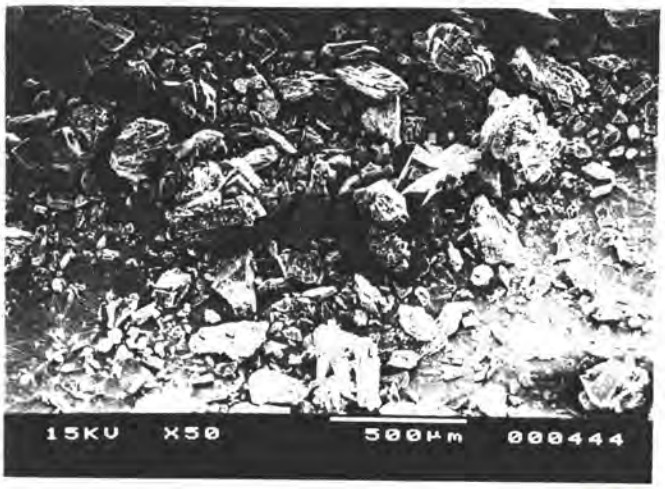

A

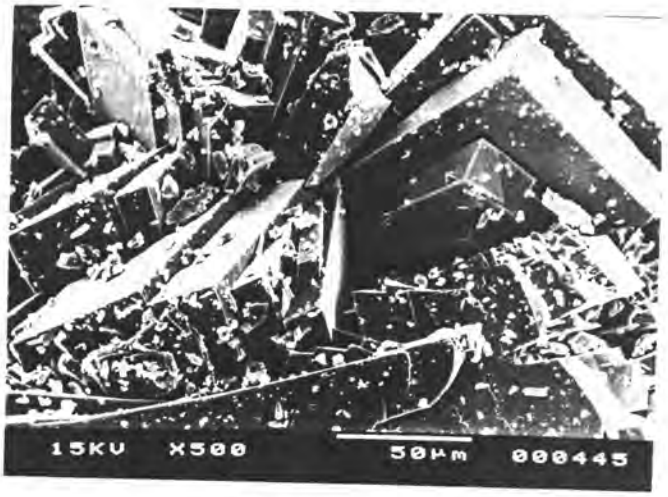

B

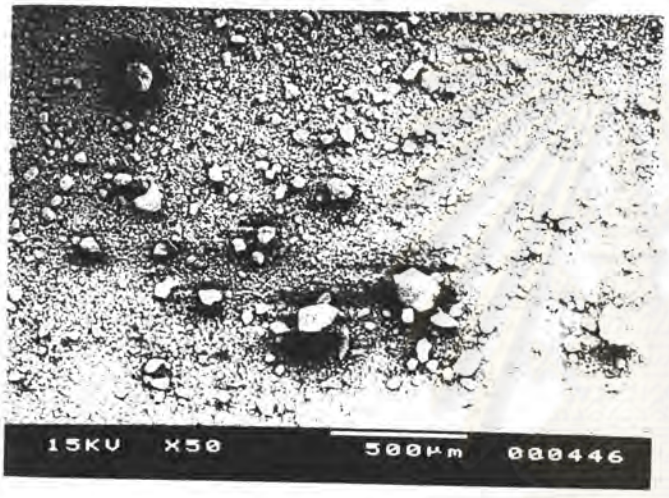

C

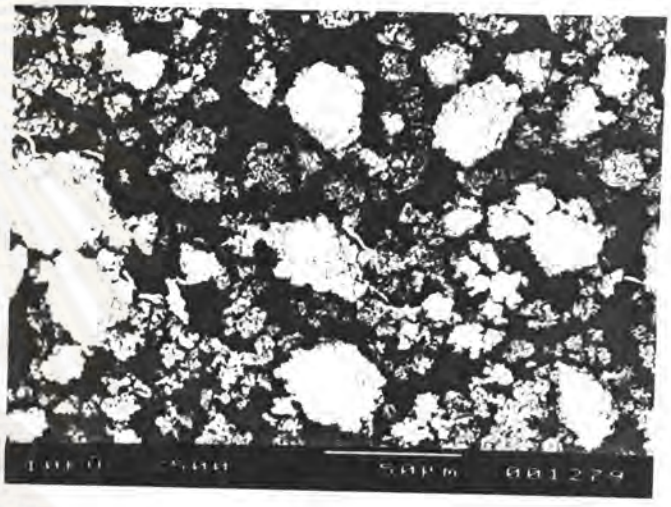

D

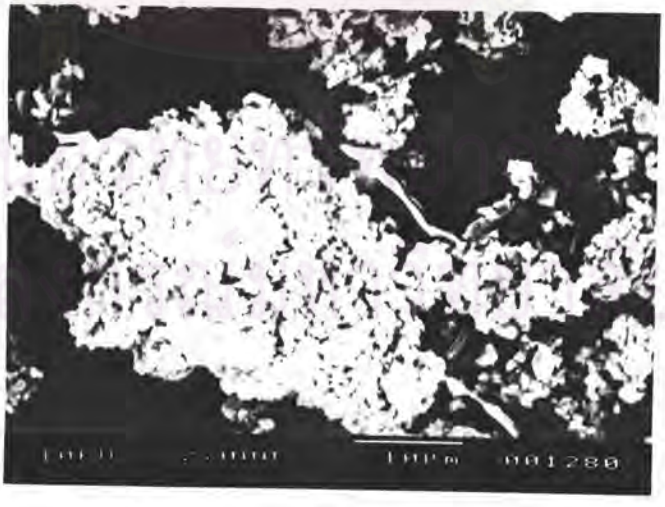

E

Figure 32 The photomicrographs of treated HCTZ
(key : A-HCTZ SM x 50, B-HCTZ SM x 500,
C-HCTZ BM x 50, D-HCTZ BM x 500, E-HCTZ BM x 2000)

A

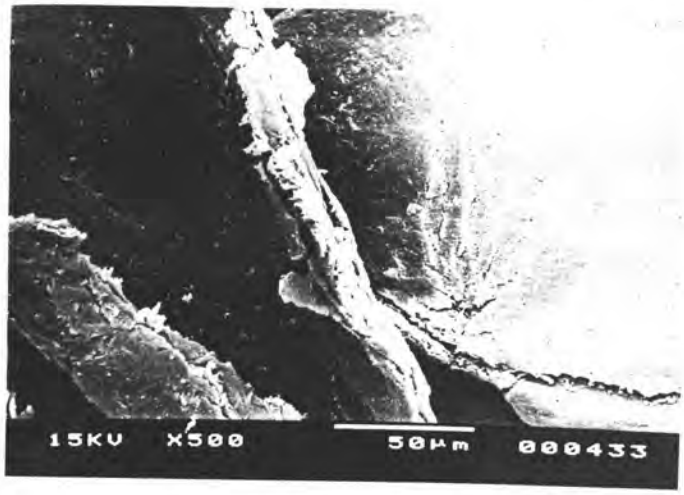

B

C

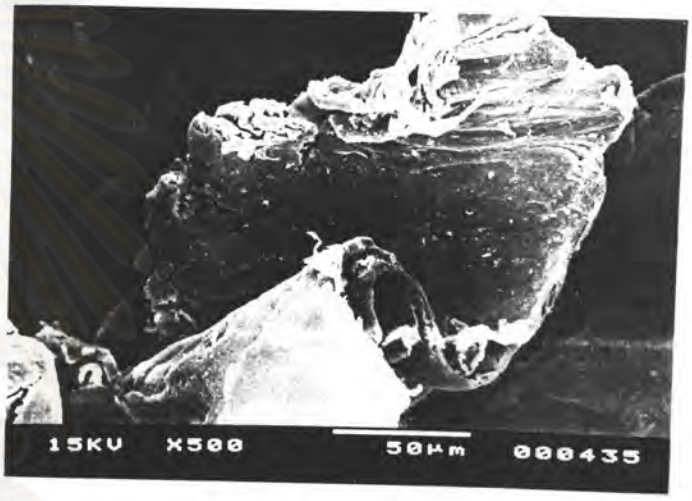

D

E

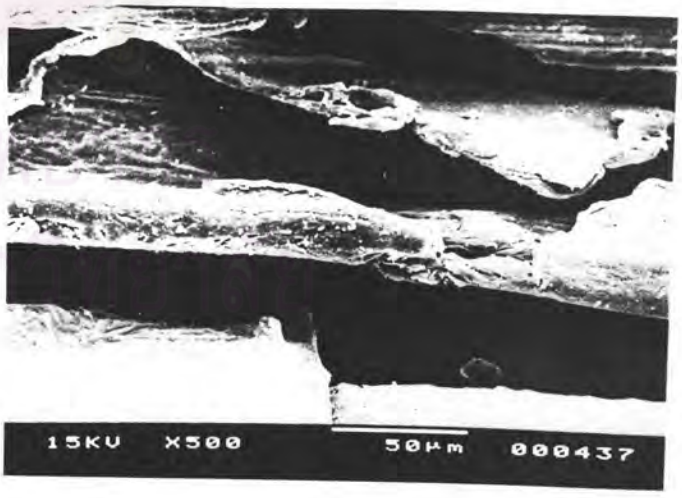

F

Figure 33 The photomicrographs of CT, CS and CSU
(key : A-CT x 50, B-CT x 500, C-CS x 50,
D-CS x 500, E-CSU x 50, F-CSU x 500)

A

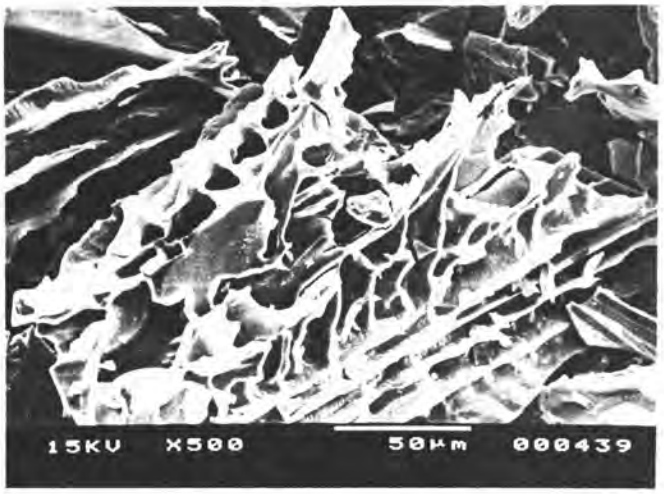

B

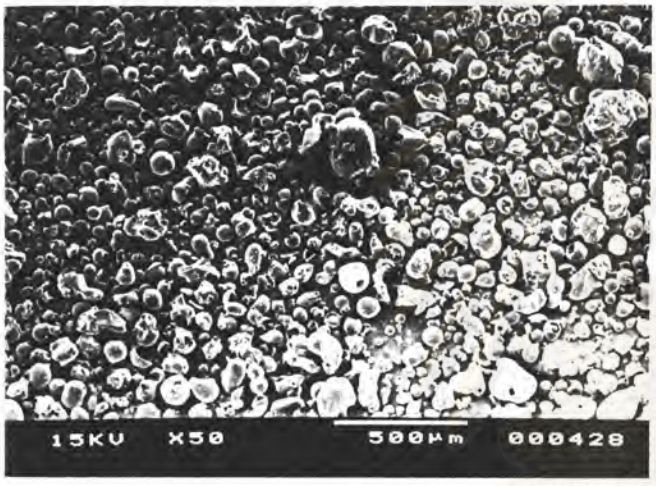

C

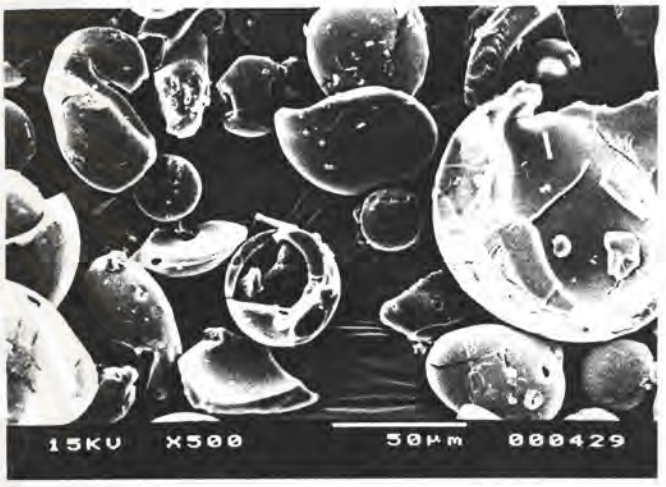

D

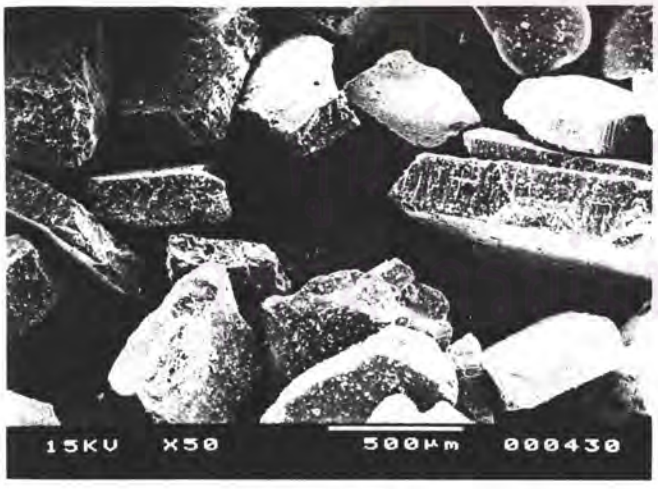

E

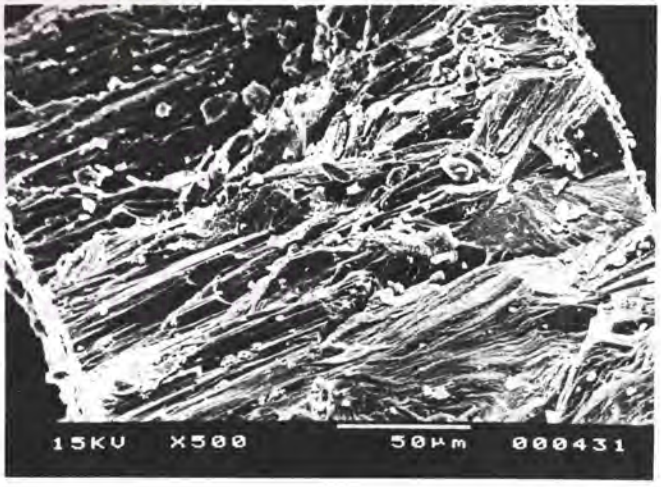

F

Figure 34 The photomicrographs of LMCS ,PVP and PEG
(key : A-LMCS x 50, B-LMCS x 500, C-PVP x 50,
D-PVP x 500, E-PEG x 50, F-PEG x 500)

about 10-100 micron. Those of PEG (E and F in Fig 34) showed irregular shaped particles in various big sizes with rough surface.

1.3 Dispersion of Physical Mixtures

The SEM photomicrographs of CT PM, CS PM, CSU PM and PVP PM in different magnification are displayed in Figures 35 (A-F) and 36 (C-D) respectively. In each system, the characteristics of neither drug nor carrier were changed. Both components were seperated. Systems of LMCS PM and PEG PM are shown in Figure 36 (A, B, E, F). The photomicrographs showed that some HCTZ broke into small paticles and deposited on the surface of both PEG or pores of LMCS and itself.

1.4 Dispersion of Kneading Mixtures

The SEM photomicrographs of CT KM, depicted in Figure 37 (A and B), showed that HCTZ crystals deposited on the curve or on the surface of carrier. Besides, the system of CS KM and CSU KM also showed the same characteristic which can be seen in Figure 37 (C, D, E, F) respectively.

For LMCS KM, the photomicrographs showed (Fig 38, A and B) that the mixtures were changed completely compared with its physical mixture. The mixture displayed irregular shape with rather smooth surface and varied in size which looked like the system of PVP KM.

The SEM photomicrographs of PVP KM are depicted in Figure 38 (C and D). The dispersion had various irregular particles shape and size, some of them were larger than the particle size of HCTZ and PVP in physical mixture and the surface of particle was rather smooth. The photomicrograph of PEG KM is illustrated in Figure 38 (E and F). The mixture changed into irregular smaller size and less rougher of surface than PEG itself, and small pieces of HCTZ adhered to its surface. The size of PEG KM is still larger than that of PVP KM.

1.5 Dispersions of Solvent Method

Figure 39 (A-F) illustrated solvent deposition system of CT, CS and CSU. The pictures showed HCTZ changed into smaller and longer crystal than the pure drug of HCTZ SM and were adhered to the surface of carrier.

A

B

C

D

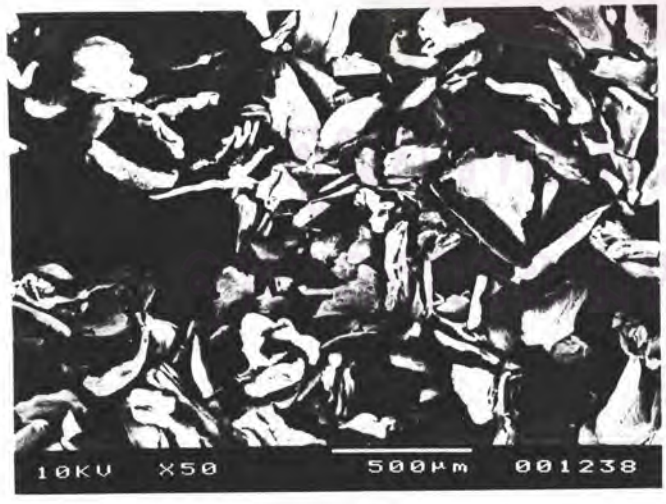

E

F

Figure 35 The photomicrographs of physical mixtures
(key : A-CT PM x 50, B-CT PM x 500, C-CS PM x 50,
D-CS PM x 500, E-CSU PM x 50, F-CSU PM x 500)

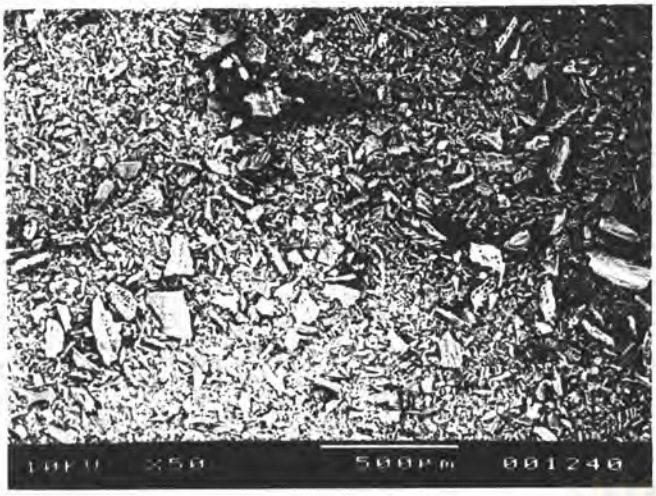

A

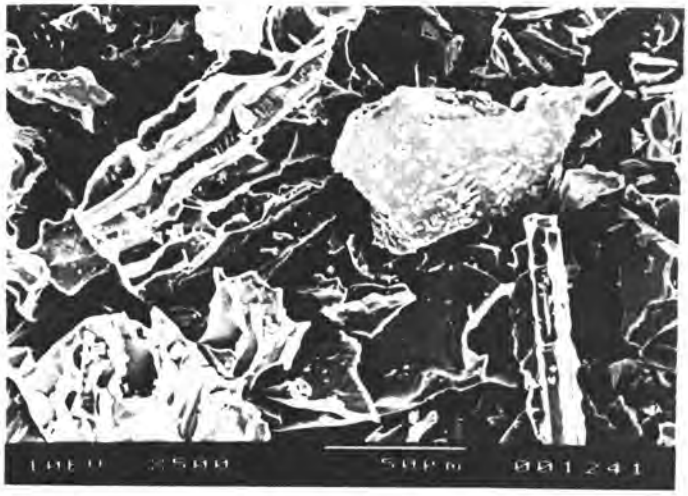

B

C

D

E

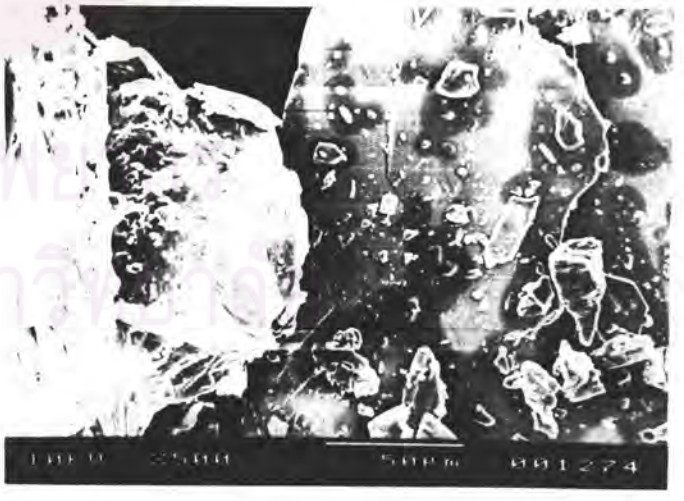

F

Figure 36 The photomicrographs of physical mixtures
(key : A-LMCS PM x 50, B-LMCS PM x 500, C-PVP PM x 50,
D-PVP PM x 500, E PEG PM x 50, F-PEG PM x 500)

A

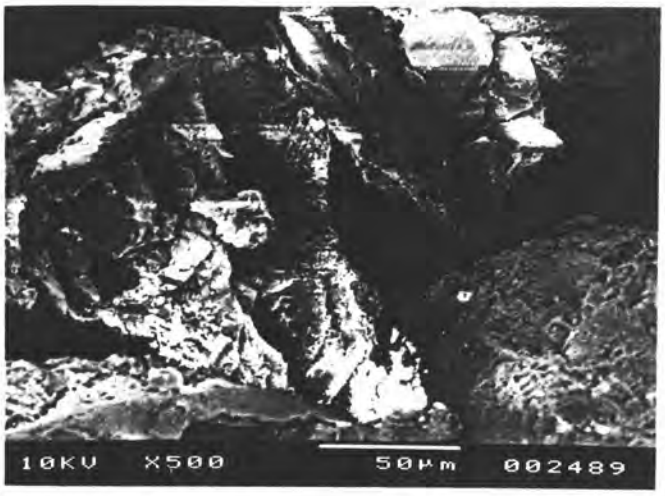

B

C

D

E

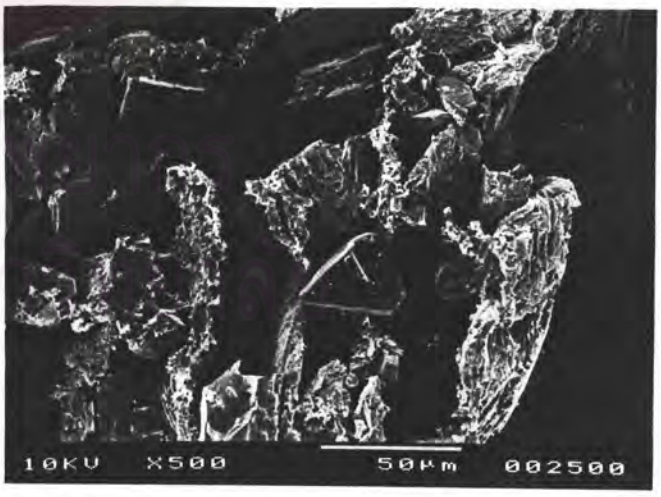

F

Figure 37 The photomicrographs of kneading mixtures
(key : A-CT KM x 50, B-CT KM x 500, C-CS KM x 50,
D-CS KM x 500, E-CSU KM x 50, F-CSU KM x 500)

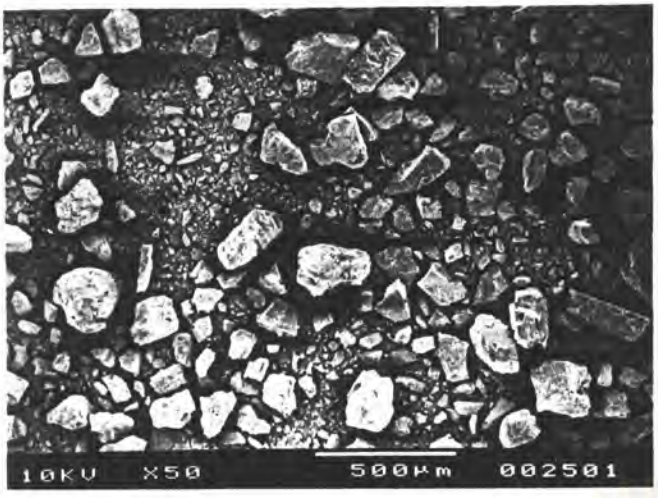

A

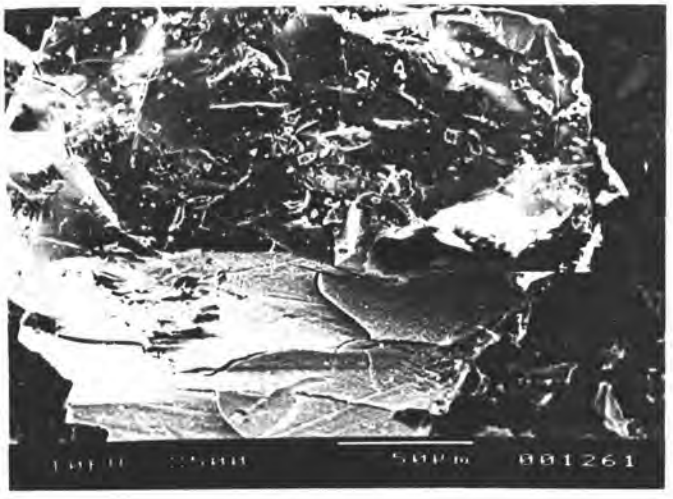

B

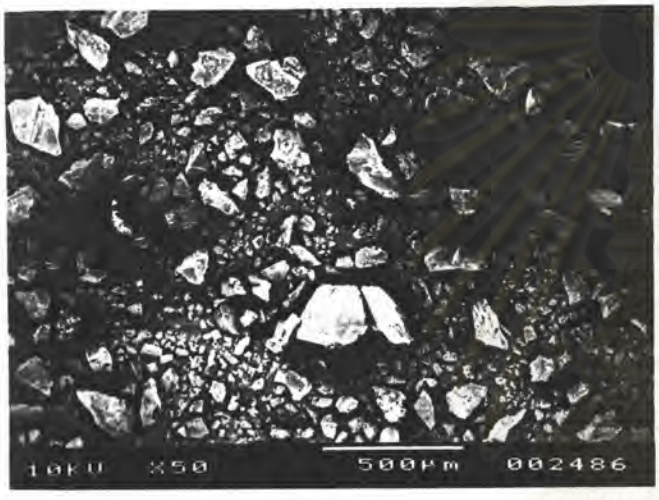

C

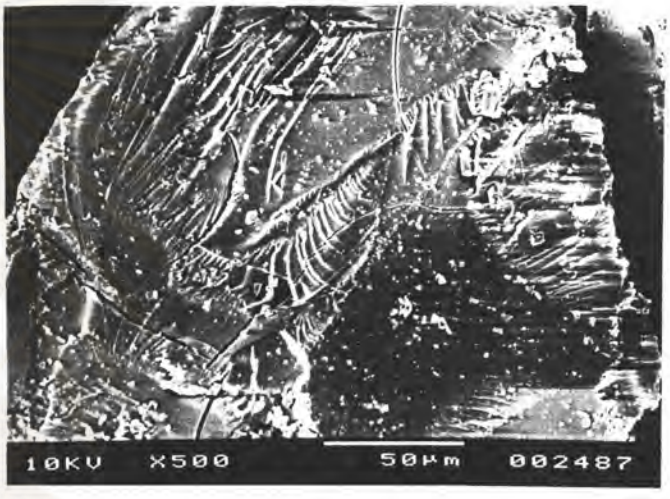

D

E

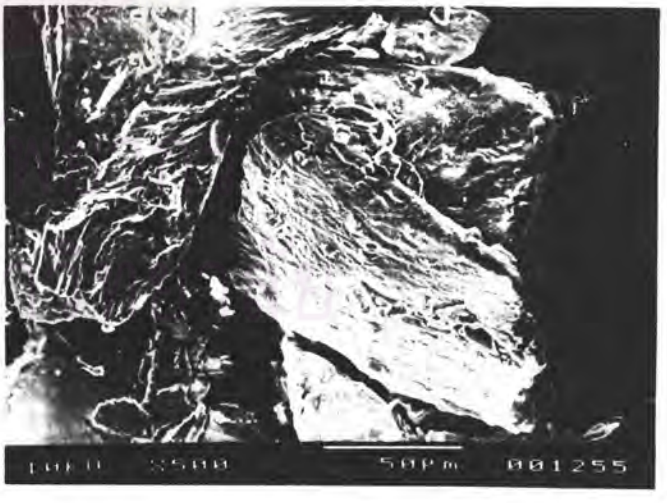

F

Figure 38 The photomicrographs of kneading mixtures
(key : A-LMCS KM x 50, B-LMCS KM x 500, C-PVP KM x 50,
D-PVP KM x 500, E-PEG KM x 50, F-PEG KM x 500)

A

B

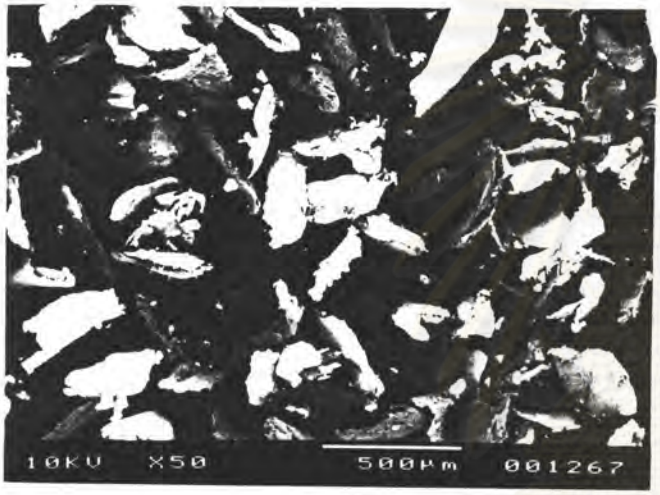

C

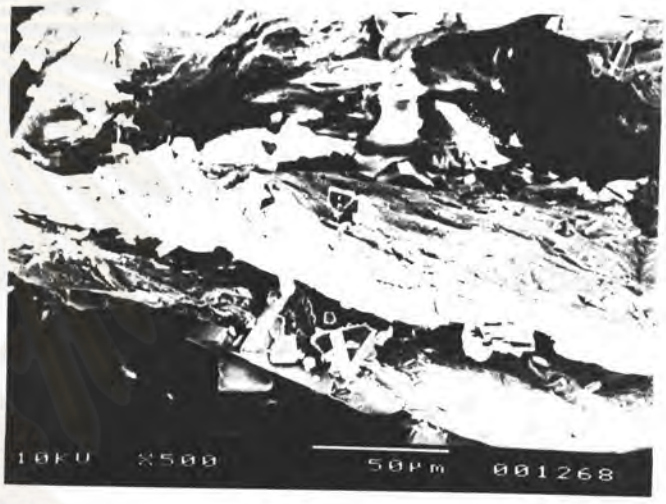

D

E

F

Figure 39 The photomicrographs of solvent deposition mixtures
(key : A - CT SMD x 50, B - CT SMD x 500, C-CS SMD x 50,
D-CS SMD x 500, E-CSU SMD x 50, F-CSU SMD x 500)

For the carrier of LMCS, its solvent dispersions and solvent deposited dispersion were compared in Figure 40 (A-D). Both mixture were different. LMCS SMD, in Figure 40 (A and B), showed that some LMCS broke into smaller particle, also HCTZ was differed from its pure drug. LMCS SM in Figure 40 (C and D), showed that new form occurred in irregular shape and rather smooth surface. The size range of those two mixtures were the same.

The microscope appearance of PVP SM (Fig 41 ; A and B) revealed that dispersion composed mainly of irregular shape with smooth surface and different size of about 50 - 200 micron. PEG SM in Figure 41(C and D) displayed the same shape and size as PVP SM, but the surface of PEG SM was rougher than that of PVP SM.

1.6 Dispersion of Ball milling method

Photomicrographs of samples ground by ball milling are shown in Figure 42-43. All systems were smaller in size range compared with itself before being treated. PVP BM was the smallest in size followed by both of LMCS BM, CT BM, CS BM and CSU BM, respectively. CT BM, in Figure 42 (A and B), was changed from its former characteristics that it was not curly and seemed to have rougher surface. Like CT BM, the same characteristic occurred with CS BM and CSU BM (Fig 42 ; C-F), whereas LMCS BM (SW & VB) displayed differently. Both mixtures of LMCS BM SW-VB (Fig 43 ; A-D) were agglomerated particles with variety in diameters ranging from 10 to 100 micron, and the size of LMCS BM-VB was smaller than LMCS BM-SW.

PVP BM, in Figure 43 (E and F) showed agglomeration of very fine particles and most of its particles were in a diameter of about 5 to 20 micron.

2. The X-ray diffractograms

The powder X-ray diffraction patterns of HCTZ, various carriers and various dispersion mixtures of 1:1 ratio were illustrated in Figure 44-48.

A

B

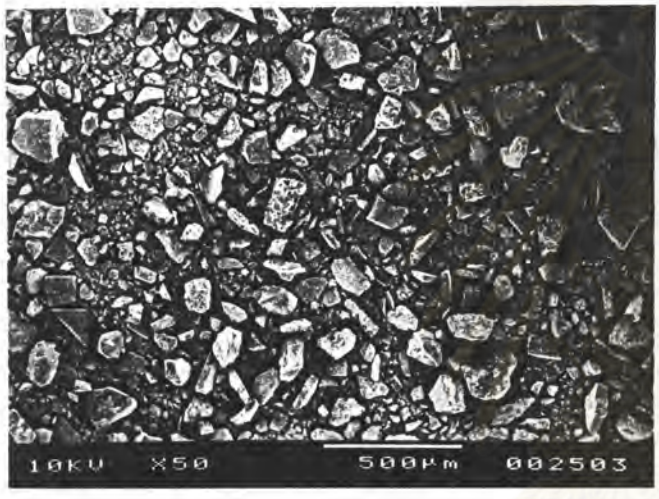

C

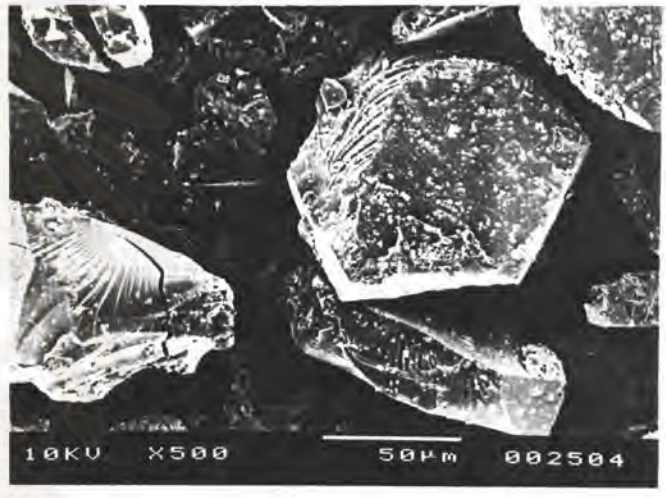

D

Figure 40 The photomicrographs of solvent and solvent deposition mixtures of LMCS (key : A-LMCS SMD x 50, B-LMCS SMD x 500, C-LMCS SM x 50, D-LMCS SM x 500)

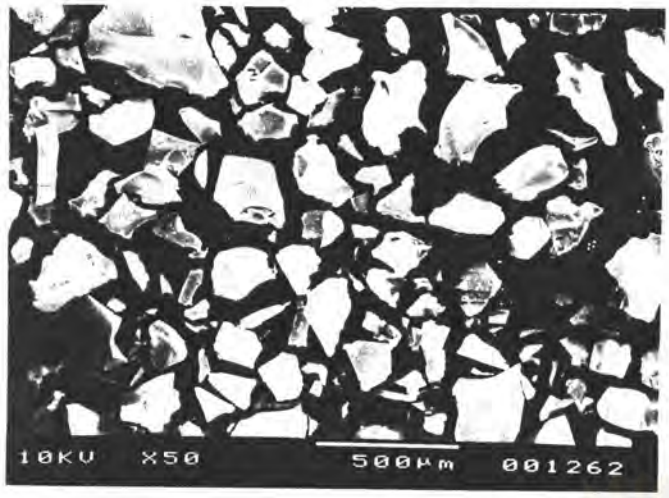

A

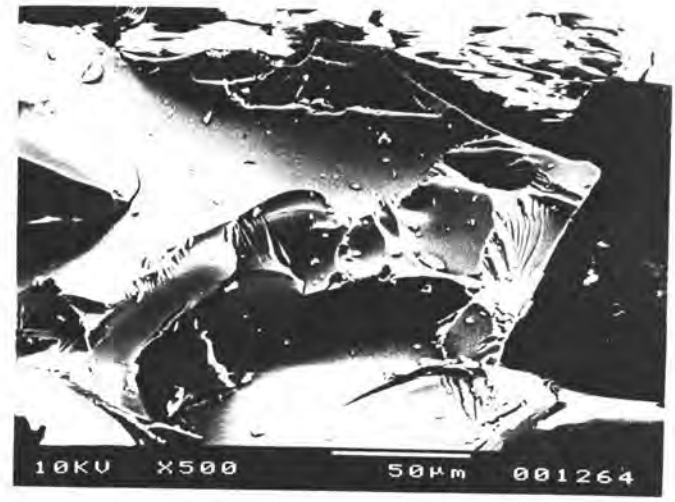

B

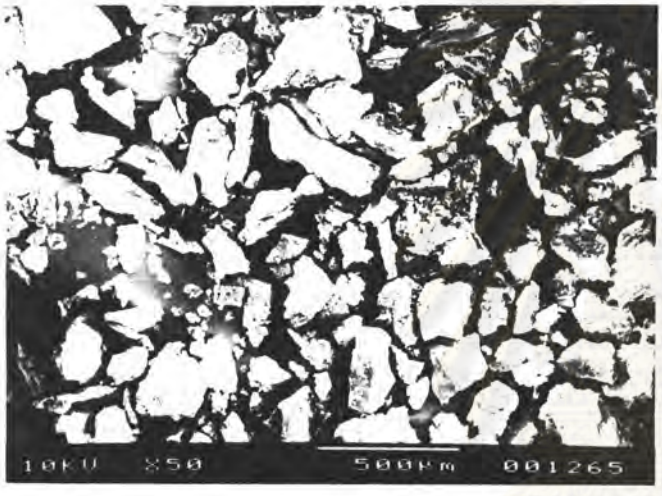

C

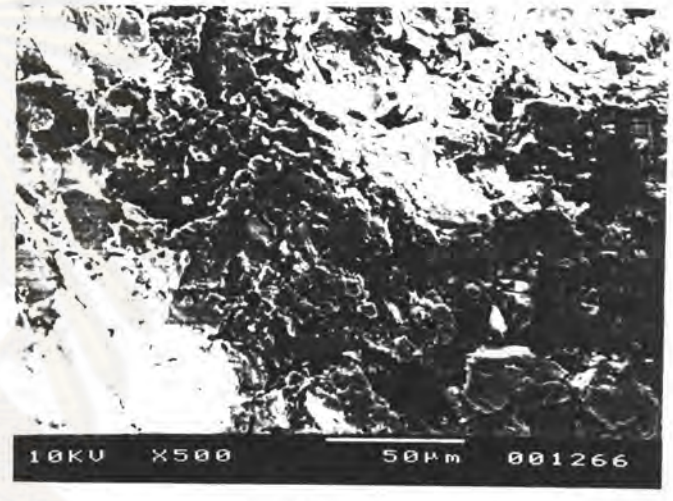

D

Figure 41 The photomicrographs of solvent mixtures
(key : A-PVP SM x 50, B-PVP SM x 500,C-PEG SM x 50,
D-PEG SM x 500)

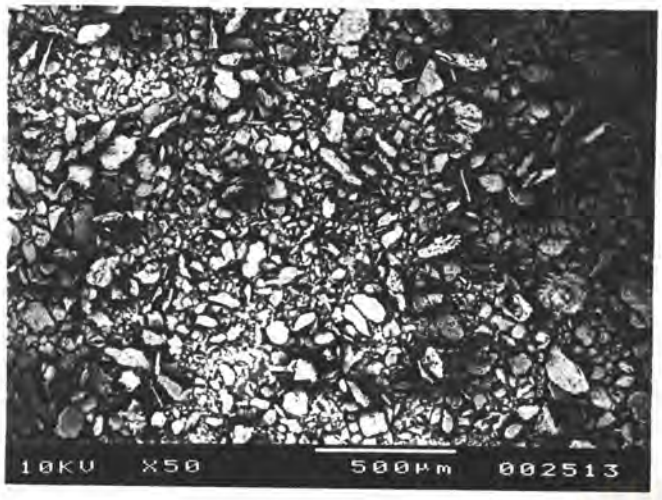

A

B

C

D

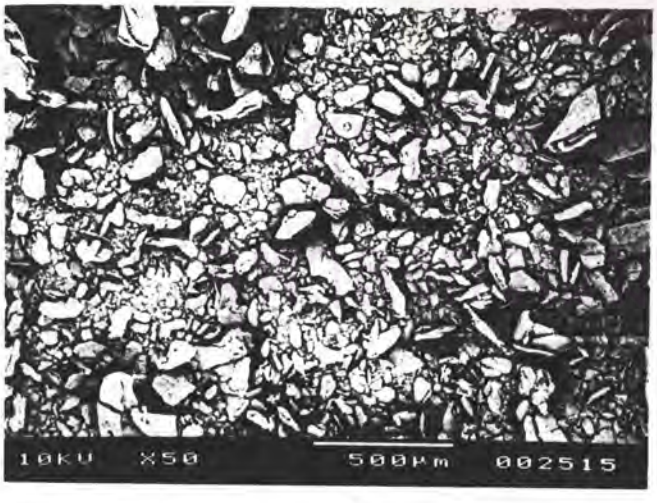

E

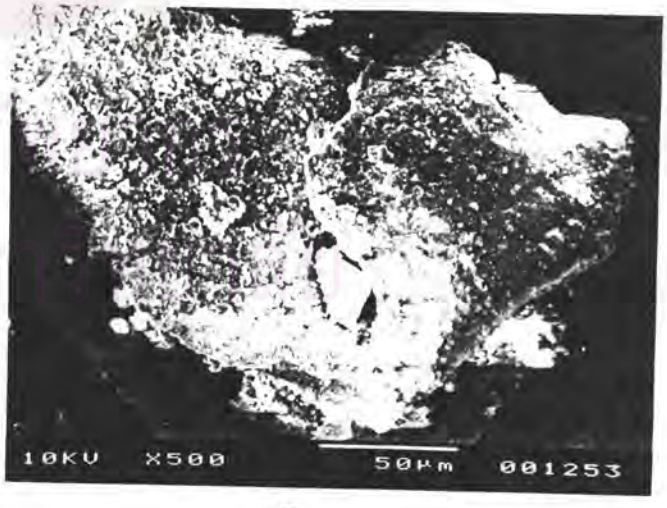

F

Figure 42 The photomicrographs of ball milling mixtures
(key : A-CT BM x 50, B-CT BM x 500, C-CS BM x 50,
D-CS BM x 500, E-CSU BM x 50, F-CSU BM x 500)

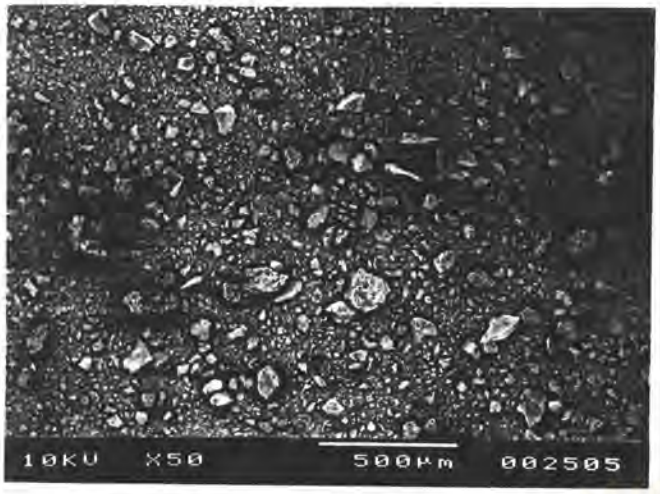

A

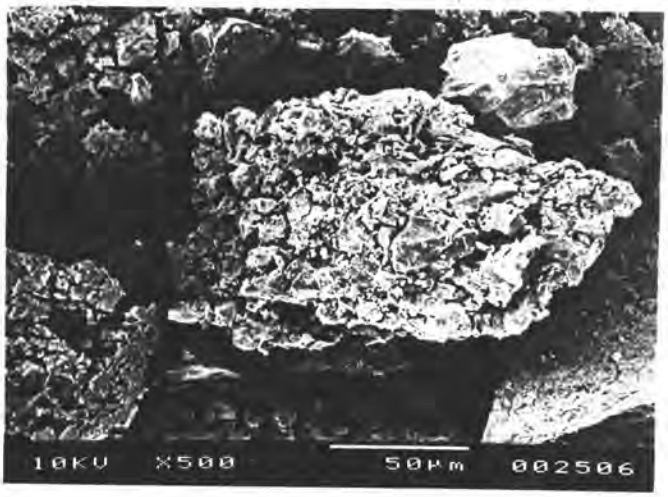

B

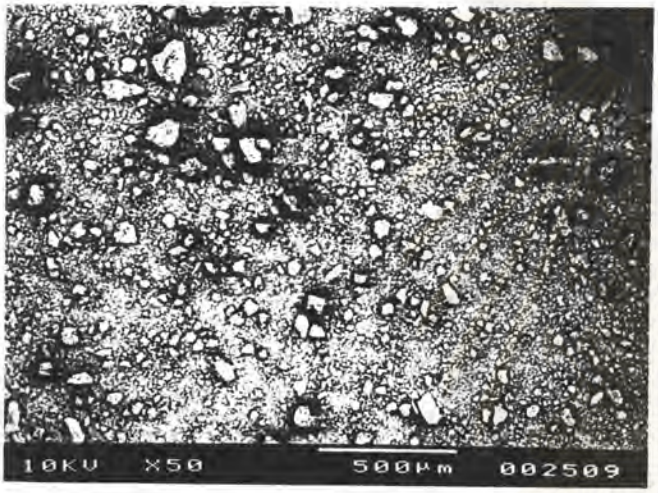

C

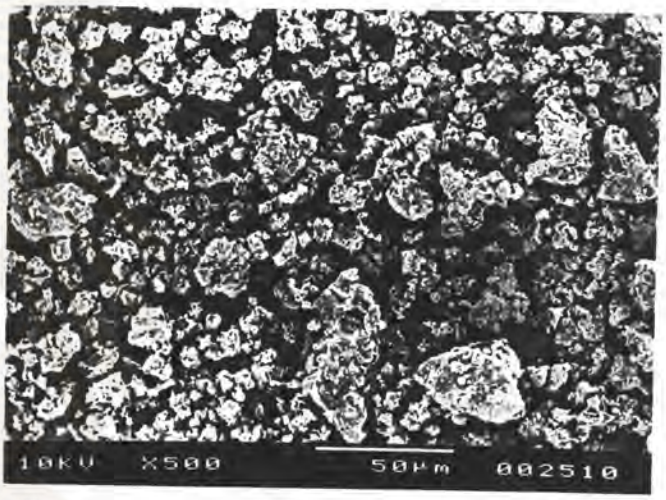

D

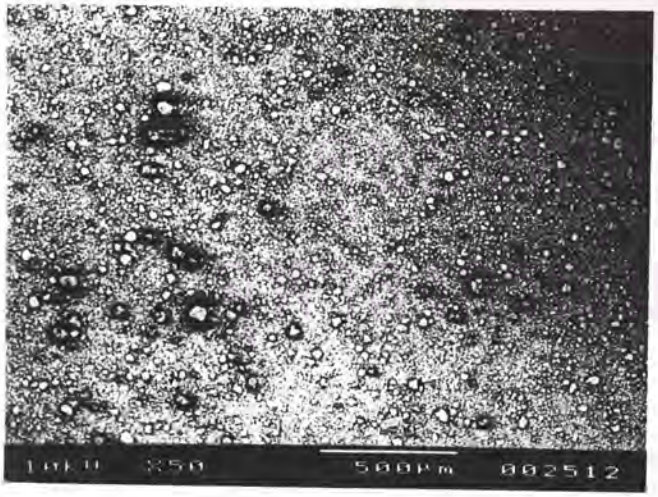

E

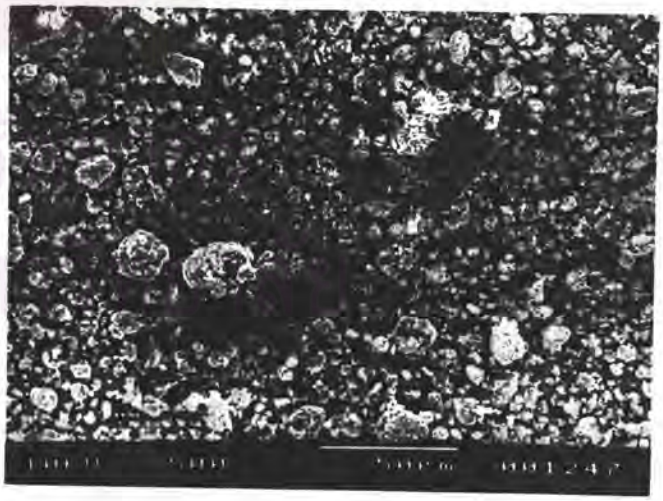

F

Figure 43 The photomicrographs of ball milling mixtures
(key : A-LMCS BM SW x 50, B-LMCS BM SW x 500,
C-LMCS BM VB x 50,D-LMCS BM VB x 500,
E-PVP BM x 50, F-PVP BM x 500)

2.1 HCTZ

The X-ray diffractograms of HCTZ and treated HCTZ were displayed in Figure 44. Major X-ray diffraction peaks of HCTZ were particularly observed at 19° and 29°. The diffractograms of HCTZ SM and HCTZ BM exhibited five major peaks; two peaks at 19° and 29° but with less intensity than those of pure drug and three new peaks at 16.5°, 21° and 24.5°. Their peaks at 19° and 21° were obviously double. HCTZ SM also showed high baseline with less peak intensity than HCTZ BM, while the latter exhibited different pattern around 38° - 40° and 45°

2.2 Carriers

The X-ray diffraction spectra of the carriers are displayed in Figure 45-48. It revealed that CT, CS, CSU and LMCS in Figures 45A, 45D, 46A, 47A were in amorphous form but with a few diffraction peaks. PVP, in Figure 48A, was also in amorphous form while PEG, in Figure 48E, was in crystalline form.

2.3 Dispersions

The X-ray diffraction spectrum of CT, CS, CSU systems are illustrated in Figures 45-46. In ball milling systems, all systems were in the same manner. The presentation of major peaks at 16.5°, 19°, 21°, 245°, 29° was the same as in HCTZ BM. However, their peak intensity was markedly less than HCTZ BM. In solvent deposition methods, all systems showed similar diffractogram and also similar to HCTZ BM. Notification was detected, CT SMD and CSU SMD showed lesser intensity of double peaks at 21° than CS SMD. The CSU KM showed mojor peaks similar to CSU BM. But intensity of some peaks was higher than those in CSU BM.

The X-ray diffraction spectra of LMCS systems are demonstrated in Figure 47. In the case of ball milling method, the diffraction patterns of both LMCS BM SW and VB were the same and also similar to that of HCTZ BM. Whereas the peak intensity was markedly lower than that of HCTZ BM. In the case of solvent method, LMCS SMD displayed the diffractogram similar to the SMD systems of CT and CSU SMD. While LMCS SM showed different pattern, the double peak at 21° was shorter and peak at 29° was changed to small single peak compared with SMD system and a new peak occurred at 22°. The diffractogram of LMCS KM also displayed major peaks like those of HCTZ BM but with less intensity.

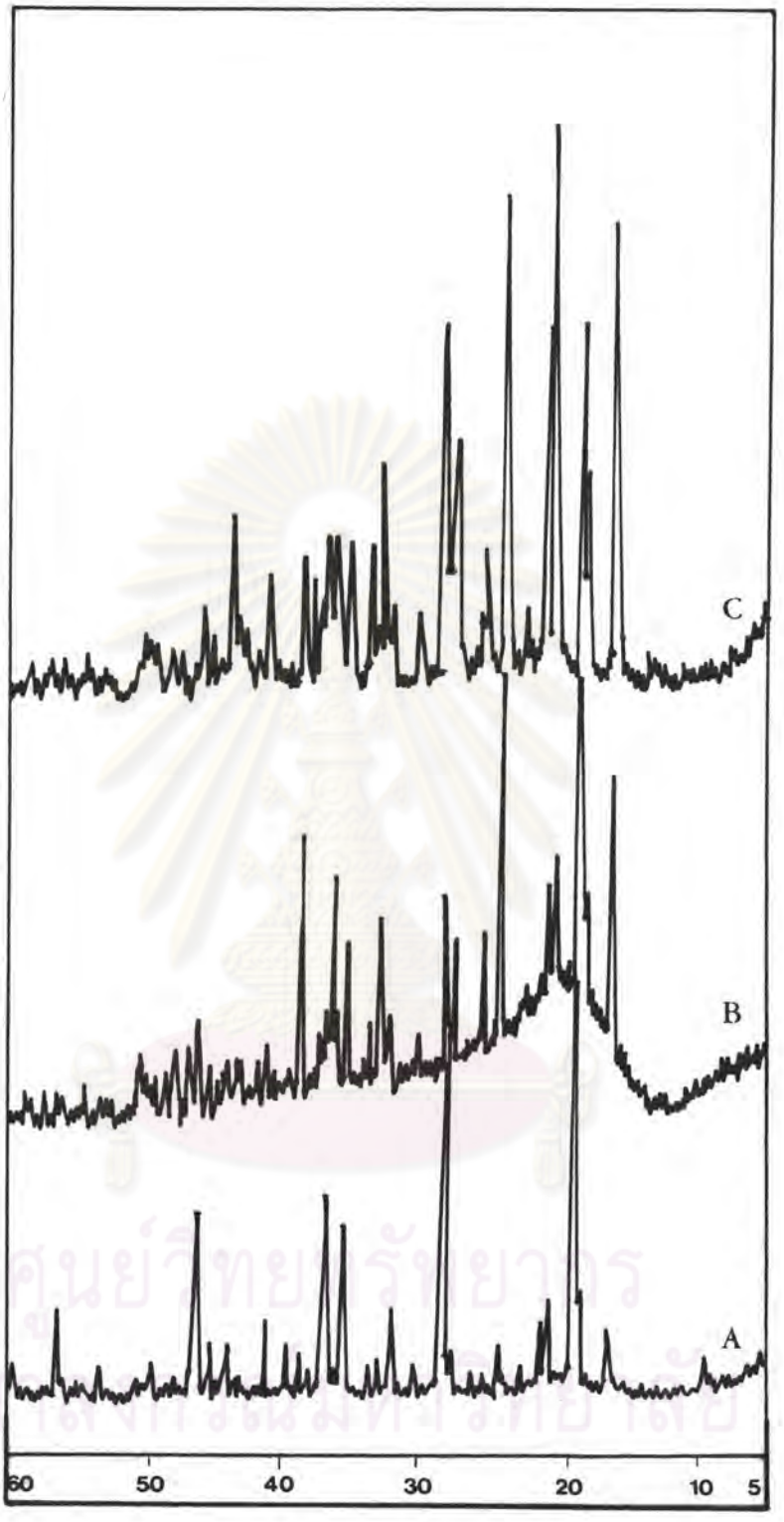

Figure 44 X-ray diffractograms of HCTZ and treated HCTZ
(key : A-HCTZ at 2000 range, B-HCTZ SM at 1000 range,
C-HCTZ BM at 1000 range)

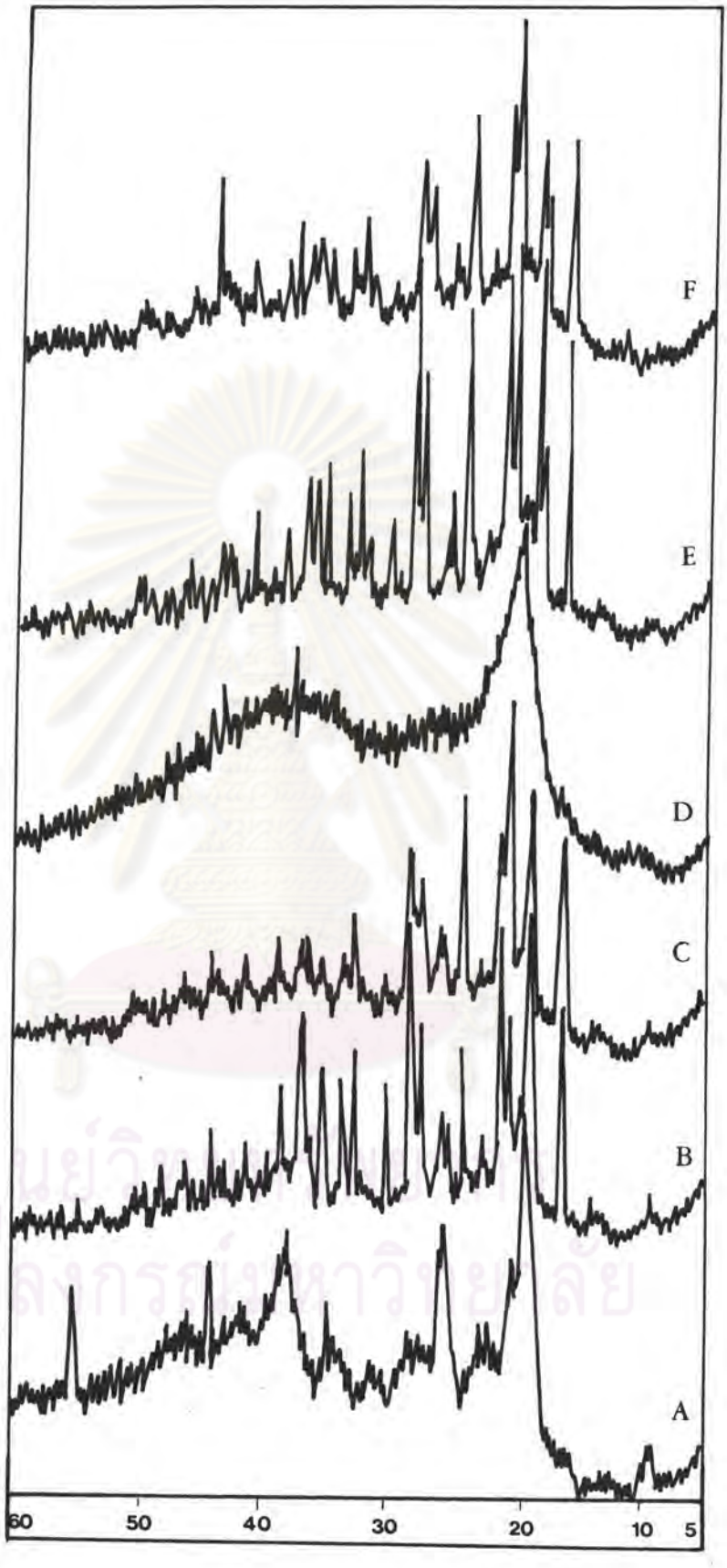

Figure 45 X-ray diffractograms of CT, CS and theirs dispersions (key : A-CT, B-CT SMD, C-CT BM, D-CS, E-CS SMD, F-CS BM, all at 1000 range)

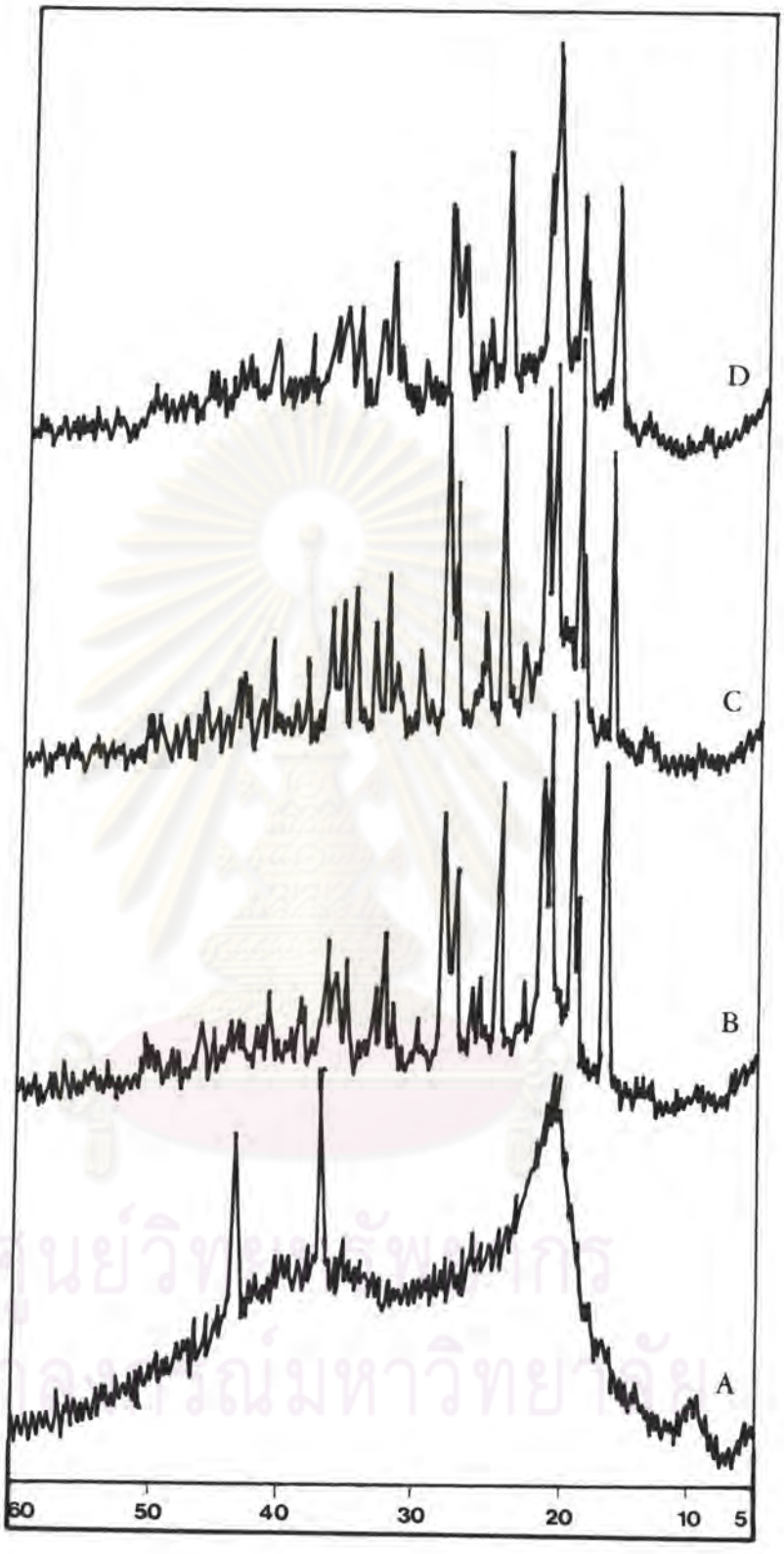

Figure 46 X-ray diffractograms of CSU and its dispersions
(key : A-CSU, B-CSU KM, C-CSU SMD, D-CSU BM
all at 1000 range)

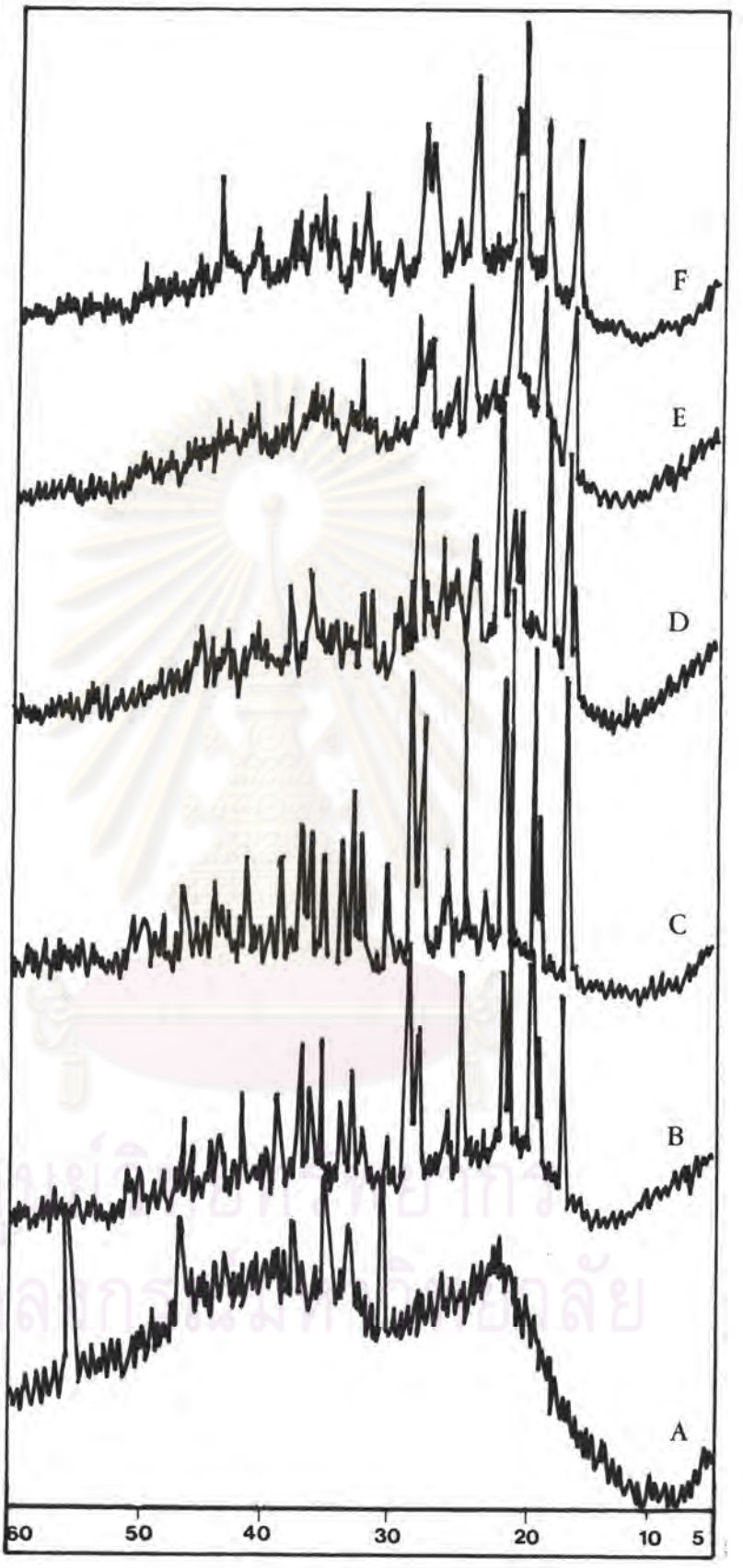

Figure 47 X-ray diffractograms of LMCS and its dispersions
(key : A-LMCS, B-LMCS KM, C-LMCS SMD, D-LMCS SM
E-LMCS BM SW, F-LMCS BM VB, all at1000 range)

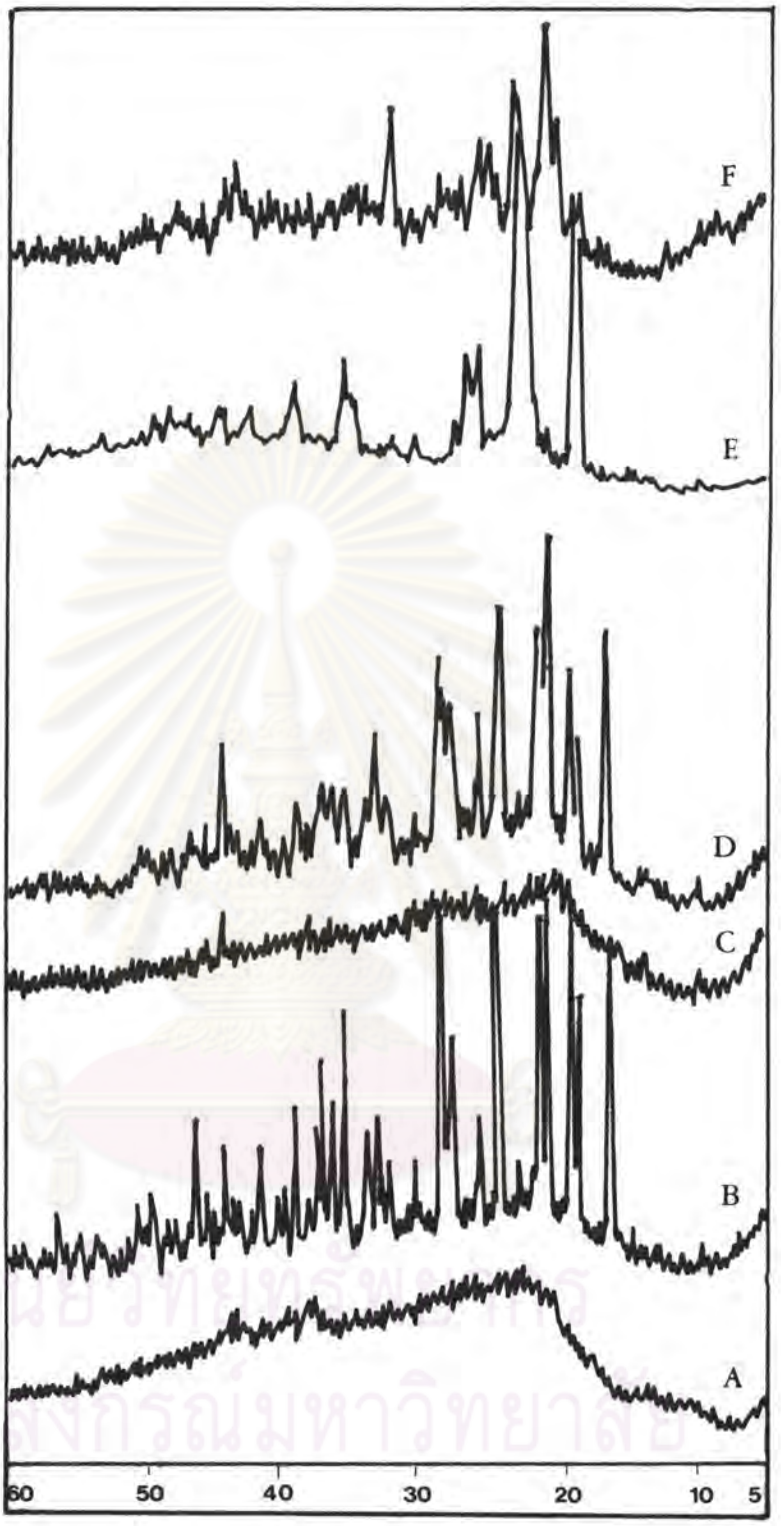

Figure 48 X-ray diffractograms of PVP, PEG and theirs dispersions
(key : A-PVP at 2000 range, B-PVP KM at 1000 range,
C-PVP SM at 1000 range, D-PVP BM at 1000 range
E-PEG at 400 range, F-PEG SM at 1000 range)

The X-ray diffraction spectra of PVP SM, in Figure 48C, exhibited absence of crystalline HCTZ peaks. PVP KM(Fig 48 B) showed the same pattern as HCTZ BM. However it showed some differences from HCTZ BM, that slightly higher intensity peaks at 19°, 29° and lesser at 16.5°, 21°, 24.5°. Moreover, the diffractogram of PVP BM (Fig 48D) also showed five major peaks as HCTZ BM but remarkably lesser of intensity peaks.

The X-ray diffraction spectra of PEG SM, in Figure 48F, compared with HCTZ and PEG alone showed different peaks and intensity. The sharp diffraction peaks attributed to HCTZ crystals were disappeared and new peaks occurred at 21° and 23.5°. This diffractogram presented new X-ray diffraction pattern.

In conclusion, ball milling method with any carrier produced five major peaks of diffractogram similar to the peaks of HCTZ BM at 16.5°, 19°, 21°, 24.5°, 29° but significantly lesser intensity peak and slightly higher baseline were detected. Kneading method also produced the X-ray diffraction similar to HCTZ BM with lower peak intensity. For solvent method, PVP SM showed amorphous form, PEG SM and LMCS SM showed new X-ray diffraction pattern. While SMD systems displayed diffractograms similar to HCTZ BM except that CT and CSU SMD exhibited remarkable lower peak intensity at 21° when compared with other carrier in SMD system.

3. DTA thermograms

The thermograms of pure HCTZ, treated HCTZ, carriers, dispersion mixtures of HCTZ and various carriers at ratio 1:1 are illustrated in Figure 49-55.

3.1 HCTZ

The thermogram of HCTZ (Fig 49) showed the characteristic melting endotherm at 272° C similar to treated HCTZ by kneading method, while that of treated HCTZ by solvent and ball milling method was at 265° C and that of treated HCTZ by swinging ball-milled was at 263° C.

3.2 Carriers

The thermogram of CT, CS and CSU displayed endothermic peak at 165° C, 158° C and 156° C respectively (Fig. 50A,51A,52A). While LMCS (Fig. 53A) showed a board melting endotherm between 130°-180° C. PVP and PEG (Fig. 54A, 55A) showed the melting endothermic at 167° C and 72° C respectively.

3.3 Dispersions

The thermogram of CT BM in Figure 50B showed two endothermic peaks, at 160° C which was nearly the same endothermic point as CT itself and a new one at 247° C.

The thermogram of CS BM in Figure 51B showed two endothermic peaks as same as CT BM, but at 168° C which was nearly the same endothermic point as CS itself and a new one at 232° C.

The thermogram of CSU KM and CSU BM are shown in Figure 52B and C. Both of them showed the same pattern of melting endothermic as CT BM or CS BM. CSU KM exhibited two endothermic peaks, at 163°C which was nearly the same endothermic point as CSU itself, and the new one at 240°C. CSU BM also showed two melting endothermic peaks but at 169°C and a broad one at 190°C.

The thermogram of LMCS KM in Figure 53B displayed a new endothermic peak at 164°C with the absence of HCTZ melting endotherm. For solvent method, both LMCS SMD and LMCS SM(Fig. 53C and D) showed the new endothermic peak at 167°C and 169°C respectively, while LMCS SM had an other small endothermic peak at 87°C. For ball milling method(Fig. 53E and F), LMCS BM (SW) showed two new endothermic peaks, a small broad peak at 68° C and a sharp one at 193°C. LMCS BM (VB) also showed two endothermic peaks, one small broad peak at 69°C and a sharp one at 154°C.

The HCTZ - PVP thermograms are illustrated in Figure 54. PVP SM exhibited two characteristic melting endotherms, at 167°C which referred to melting endotherm of PVP but decreased in intensity, and the new one at 189°C. PVP BM also showed melting endotherm of PVP at 169°C. No melting endotherm of HCTZ was observed in both thermograms.

The thermogram of PEG - SM as shown in Figure 55 displayed two new endothermic peaks, a small broad peak around 53° C and a sharp one at 89° C, which were different from those of pure HCTZ and PEG thermograms. All melting point of HCTZ, treated HCTZ, carriers and various dispersions were summarized in Table 5.

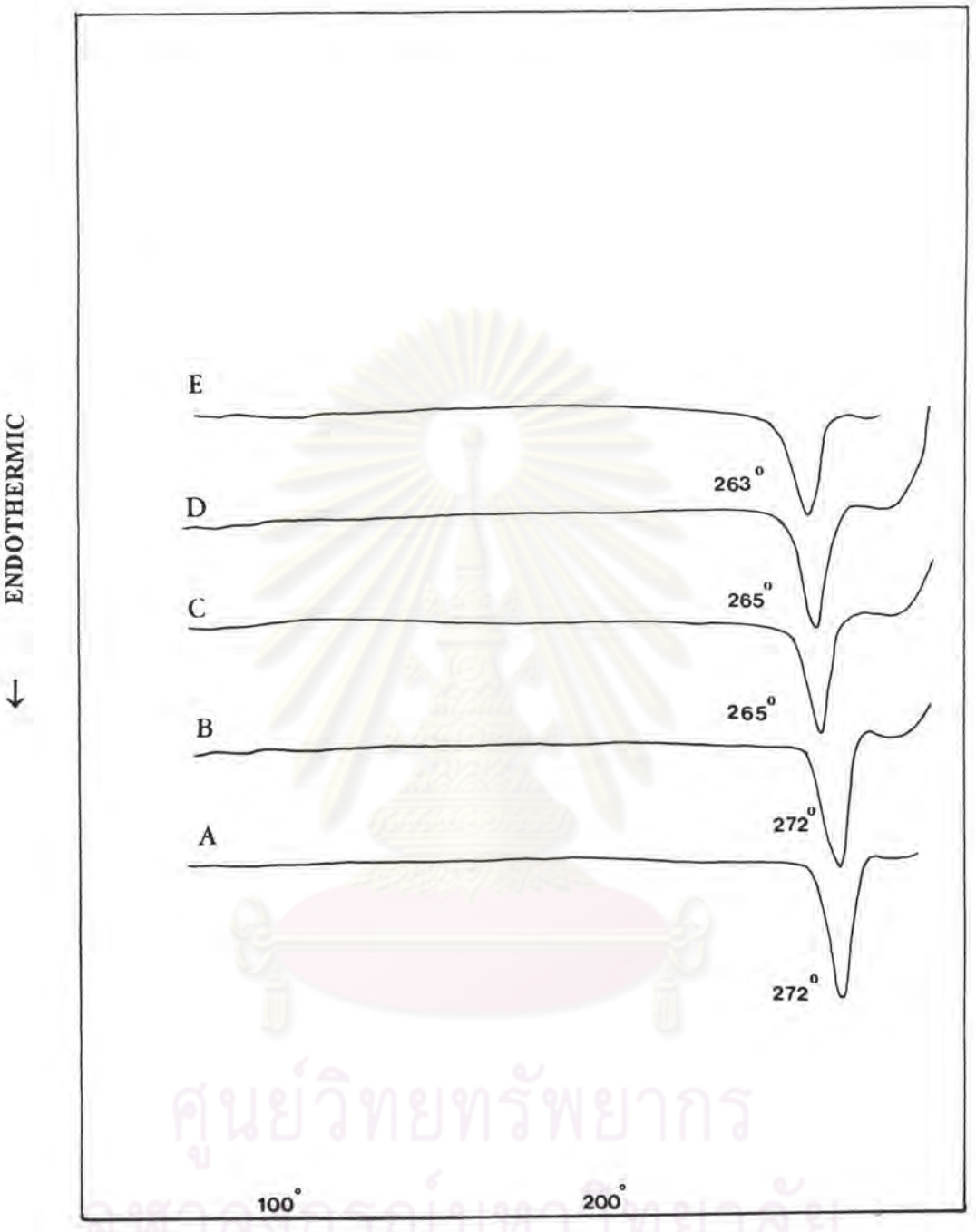

Figure 49 DTA thermograms of HCTZ and treated HCTZ (key : A-HCTZ, B-HCTZ KM, C-HCTZ SM, D-HCTZ BM, E-HCTZ BM-SW)

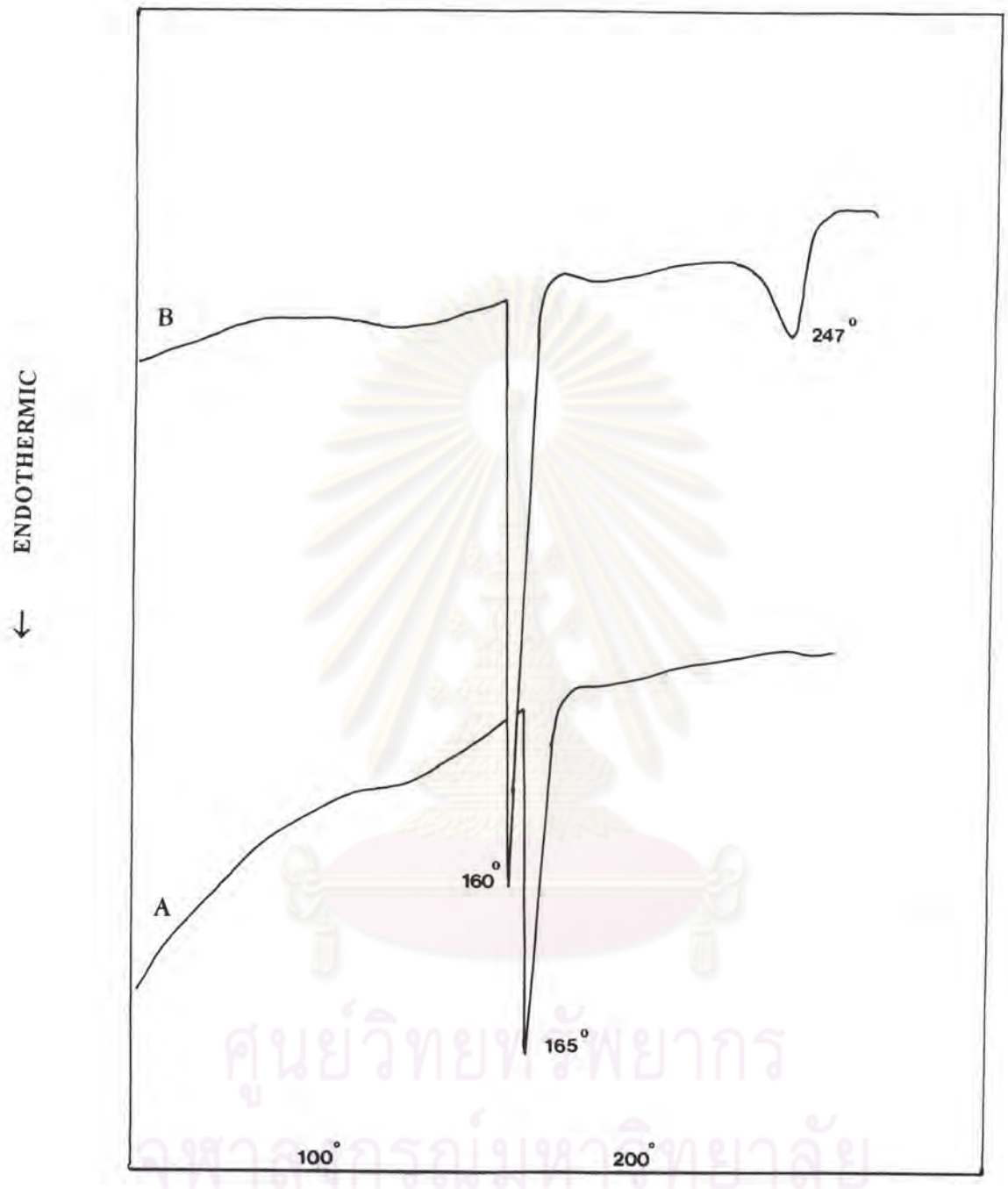

Figure 50 DTA thermograms of CT and its dispersions
(key : A-CT, B-CT BM)

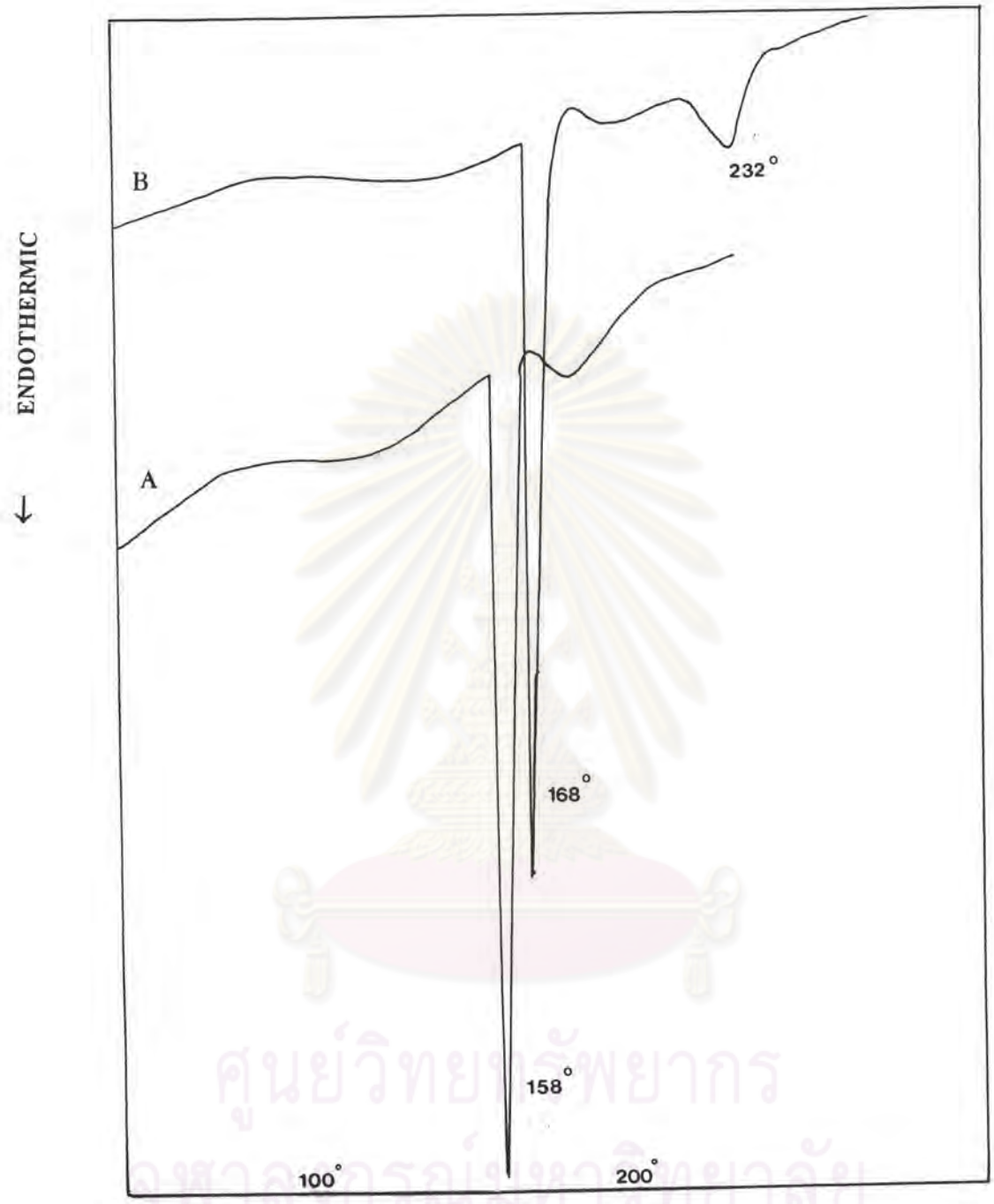

Figure 51 DTA thermograms of CS and its dispersions
(key : A-CS, B-CS BM)

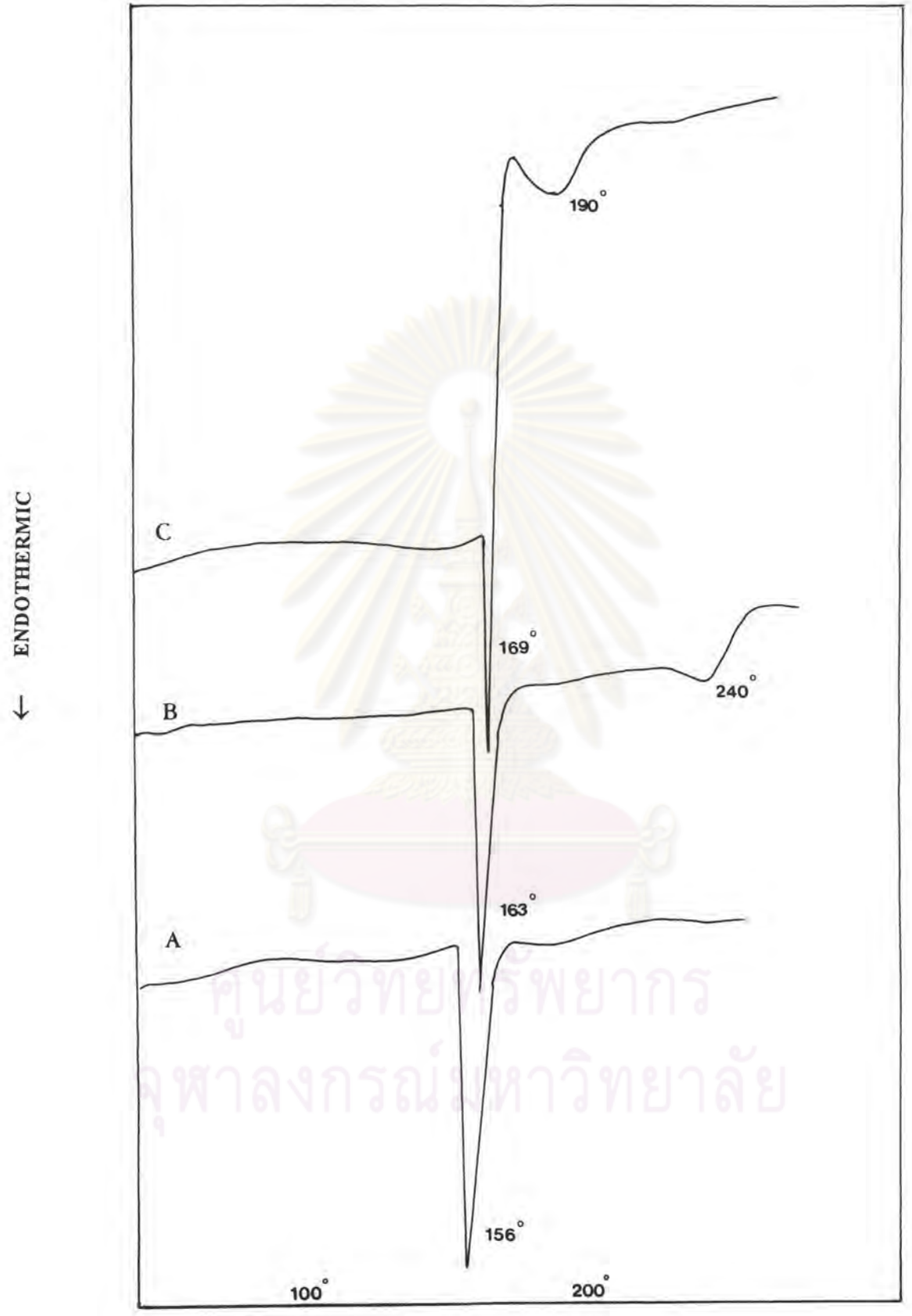

Figure 52 DTA thermograms of CSU and its dispersions
(key : A-CSU, B-CSU KM, C-CSU BM)

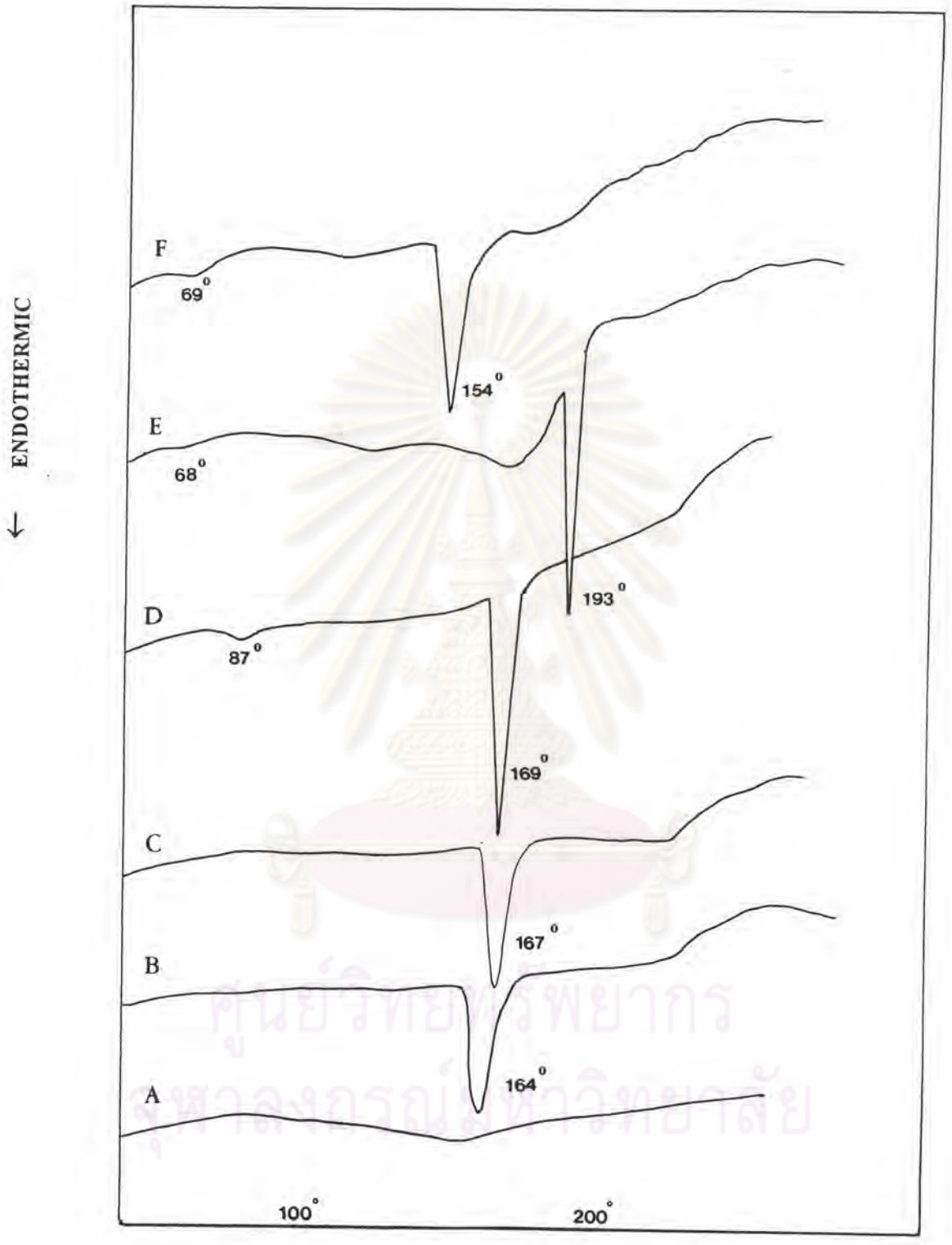

Figure 53 DTA thermograms of LMCS and its dispersions
(key : A-LMCS, B-LMCS KM, C-LMCS SMD
D-LMCS SM, E-LMCS BM SW, F-LMCS BM VB)

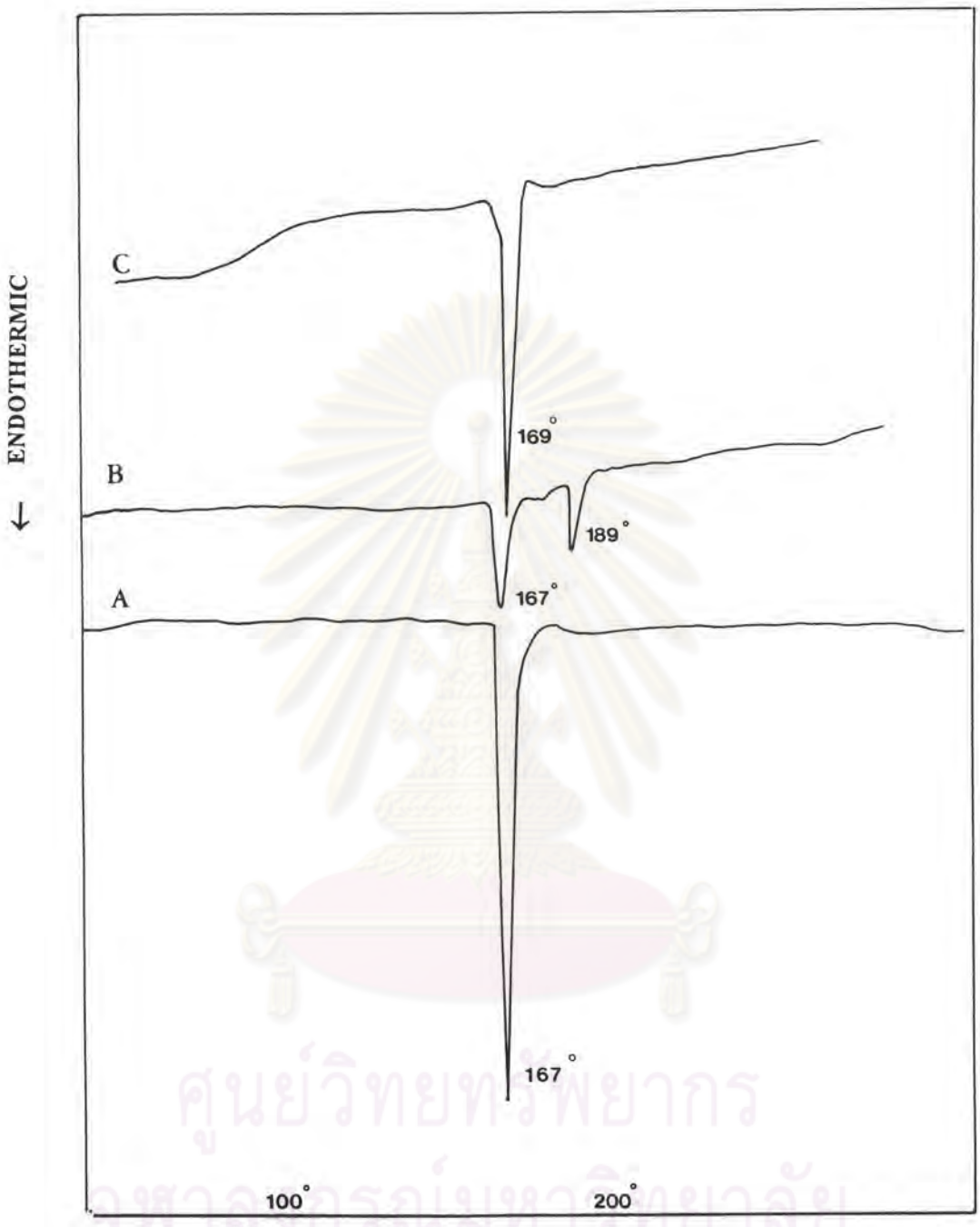

Figure 54 DTA thermograms of PVP and its dispersions
(key : A-PVP, B-PVP SM, C-PVP BM)

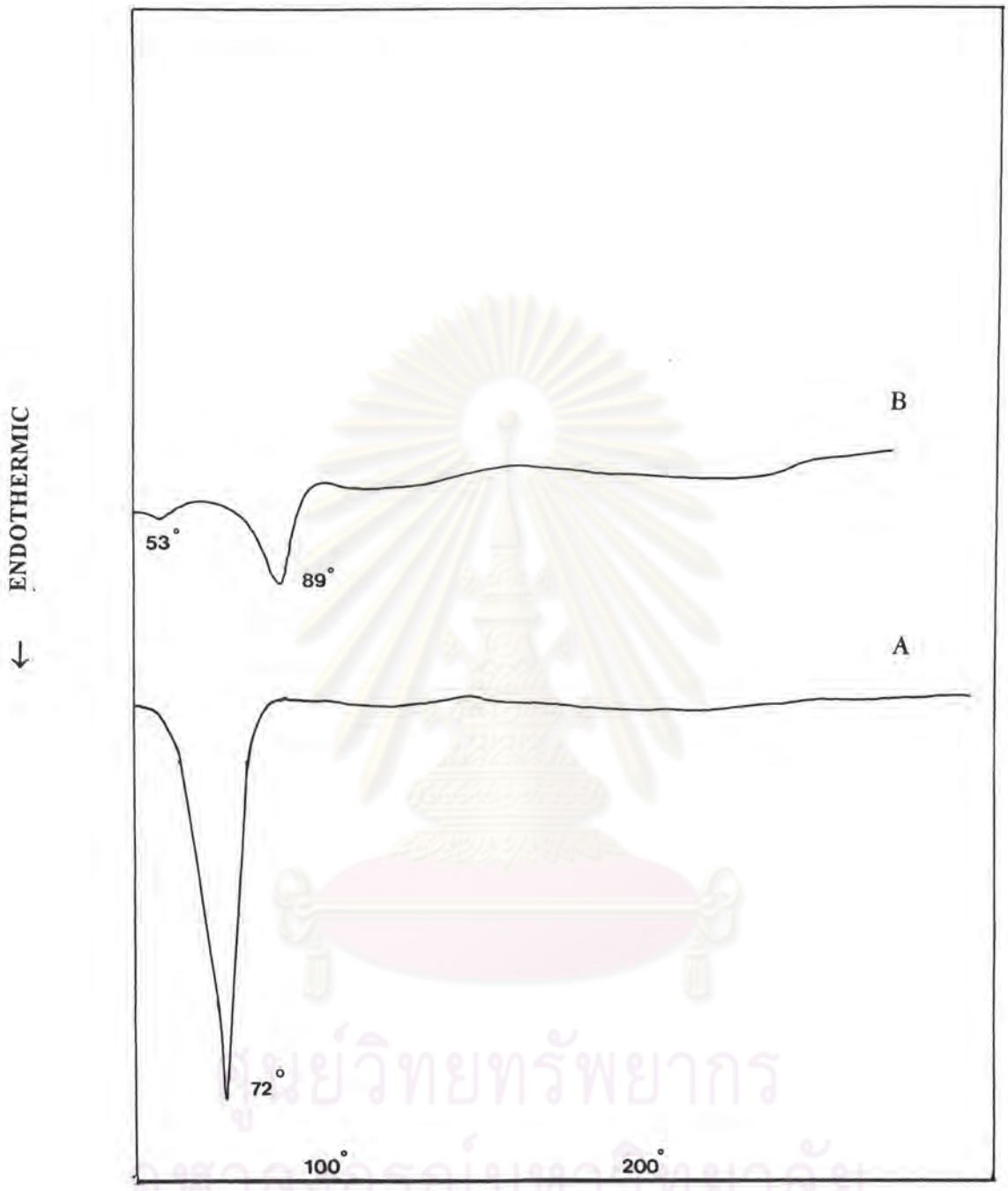

Figure 55 DTA thermograms of PEG and its dispersions
(key : A-PEG, B-PEG SM)

Table 5 The summary of melting point peaks of HCTZ, carriers and various dispersions.

Sample	Melting point peak (celcius degree)		
	<100	100-200	>200
HCTZ	-	-	272
HCTZ KM	-	-	272
HCTZ SM	-	-	265
HCTZ BM	-	-	265
HCTZ BM SW	-	-	263
CT	-	165	-
CT BM	-	160	247
CS	-	158	-
CSU	-	156	-
CSU KM	-	163	240
CSU BM	-	169,190 B	-
LMCS	-	130-180 B	-
LMCS KM	-	164	-
LMCS SMD	-	167	-
LMCS SM	87 SB	169	-
LMCS BM SW	68 SB	193	-
LMCS BM VB	69 SB	154	-
PVP	-	167	-
PVP SM	-	167, 189	-
PVP BM	-	169	-
PEG	72	-	-
PEG SM	53 SB 89	-	-

Note B : Broad peak
SB : Small broad peak

4. The IR Spectra

4.1 HCTZ

The IR spectrum of HCTZ is presented in Figure 57A. The IR spectra of HCTZ showed major peaks of : NH stretching at 3370, 3270, 3170 cm^{-1} which indicated NH stretching of NH + NH_2 group; C=C stretching at 1600, 1500, 1520 cm^{-1} which indicated C=C stretching of heterocyclic ring system ; and SO_2 stretching at 1320, 1180, 1150 cm^{-1} which indicated SO_2 stretching of SO_2 group (Deppeler, 1981)

4.2 Carriers

The IR spectrum of carriers of CT, CS, CSU and LMCS are illustrated in Figure 56.

The IR spectrum of CT showed major peaks of C=O stretching at 1650 and 1550 cm^{-1} which were the most significant parts of the spectra showing the amide bands. The peak at 1650 cm^{-1} indicated C=O stretching of amide I group and also at 1550 cm^{-1} of amide II group. These absorption bands referred to the carbonyl and amide interactions of the acetamide group in chitin. Another interesting peaks at 3450 cm^{-1} and 3250 cm^{-1} which were the peaks of O-H stretching and N-H stretching (Takai et al ., 1989).

The IR spectrum of CS showed major peak of C=O stretching at 1650 cm^{-1}. This spectrum differed from that of chitin in the absence of 1550 cm^{-1} and 3250 cm^{-1} bands. In contrast, CSU showed different IR spectra from CS, a shoulder peak at 1650 cm^{-1} and boarder peak around 3000 cm^{-1} to 3500 cm^{-1} than CS. The IR spectrum of LMCS has the same pattern of CS spectra except the peak at 1650 cm^{-1} of LMCS spectra showed little shoulder peak but was different from the shoulder of CSU peak.

4.3 Dispersions

The IR spectra of CT BM, CS BM, LMCS KM, and LMCS SM are illustrated in Figure 57(B-E).

The IR spectra of 1:1 CT BM, Figure 57B, showed the combination of peaks of CT and HCTZ. This combination was confirmed by peaks at 1600 and 1520 cm^{-1}. Other interesting peaks indicated HCTZ peaks.

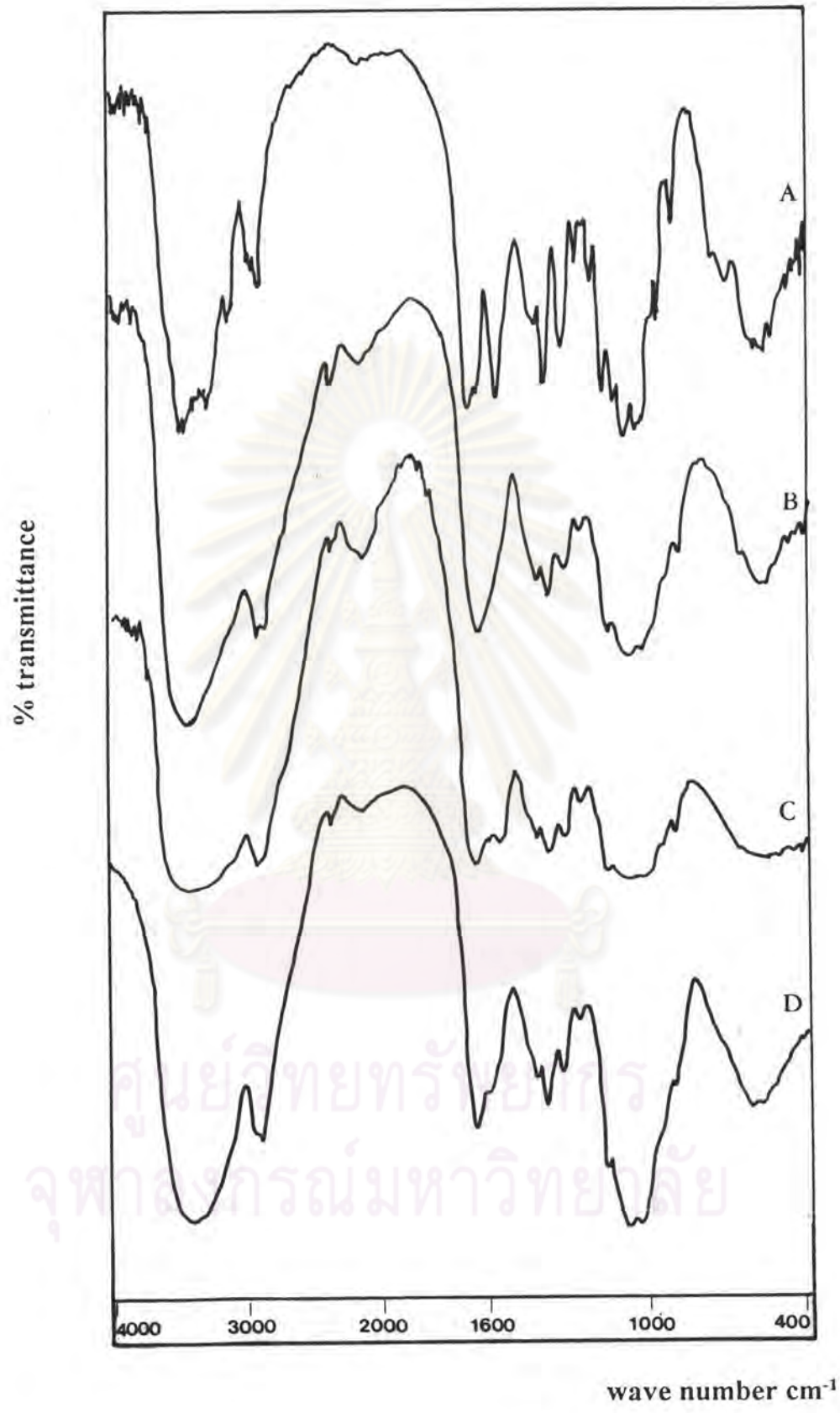

Figure 56 IR spectra of carriers (key : A-CT, B-CS, C-CSU, D-LMCS)

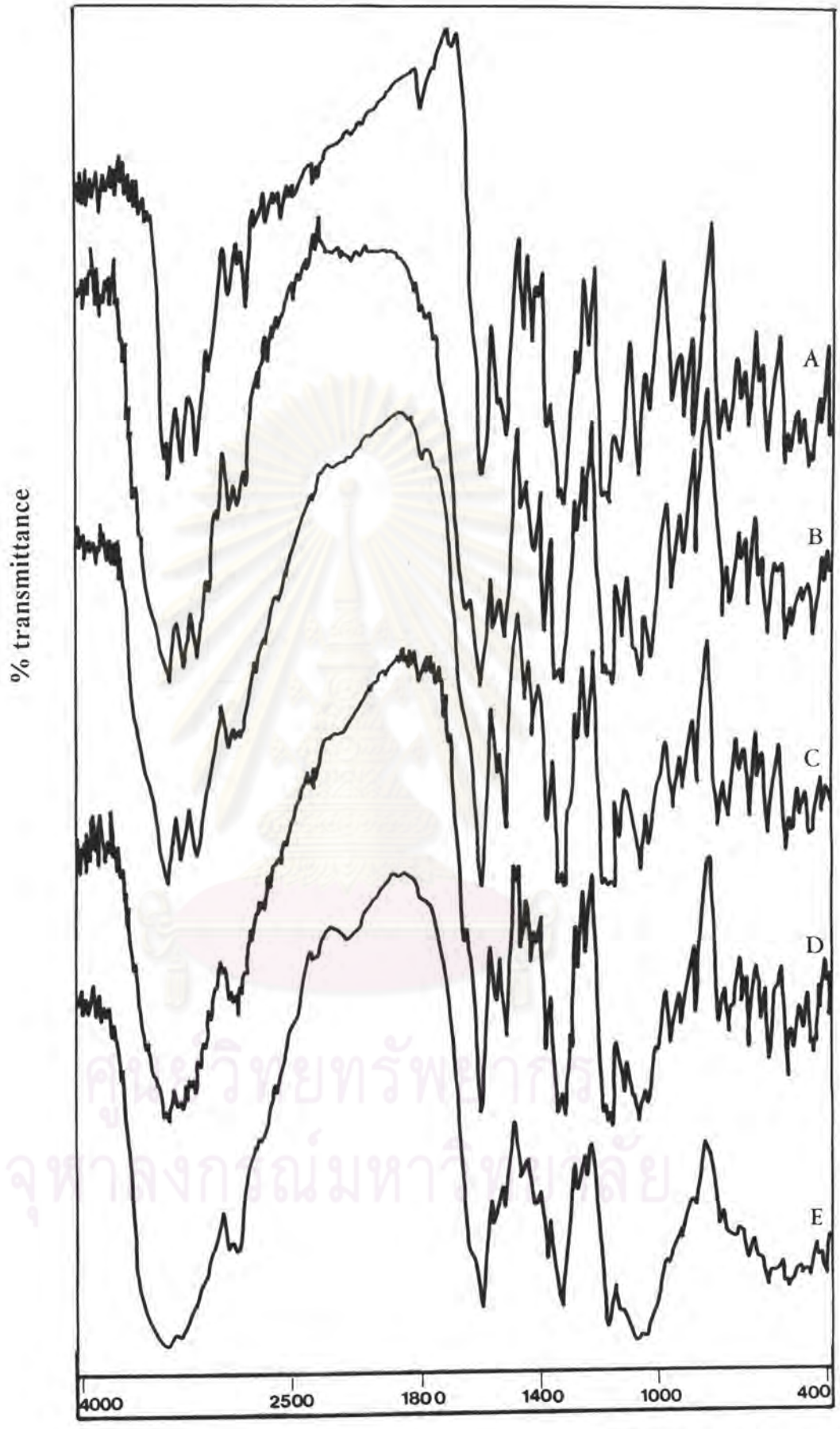

Figure 57 IR spectra of HCTZ and some dispersions
(key : A-HCTZ, B-CT BM (1:1), C-CS BM (1:1)
D-LMCS KM (1:1), E-LMCS SM (1:2)

The IR spectra of 1:1 CS BM (Figure 57C) and 1:1 LMCS KM (Figure 57D) showed the same interesting peaks as 1:1 CT BM which indicated the combination of the drug and the carrier. Whereas the IR spectra of 1:2 LMCS SM (Figure 57E) showed shorter peak of HCTZ at 1520 cm^{-1} and the peak at 1600 cm^{-1} with shoulder at 1650 cm^{-1} due to the increase of carrier ratio. All mentioned dispersions showed no chemical interactions between drug and carrier.